2020

Sex and ancestry estimation using computed tomography: a comparison of the reliability of digital versus physical data collection

BOSTON UNIVERSITY

SCHOOL OF MEDICINE

Thesis

SEX AND ANCESTRY ESTIMATION USING COMPUTED TOMOGRAPHY: A COMPARISON OF THE RELIABILITY OF DIGITAL VERSUS PHYSICAL DATA COLLECTION

by

ELENA JANOWIAK

B.A., University of Wisconsin-Madison, 2017

Submitted in partial fulfillment of the

requirements for the degree of

Master of Science

2020

Approved by

First Reader ______________________________

Sean D. Tallman, Ph.D., RPA
Assistant Professor of Anatomy and Neurobiology and Anthropology

Second Reader ______________________________

Tara Moore, Ph.D.
Associate Professor of Anatomy and Neurobiology

ACKNOWLEDGMENTS

I would like to thank my thesis committee for their gracious and reliable assistance and support as I completed this research during the stress of these unprecedented global events, namely the COVID-19 outbreak and the Black Lives Matter protests. I would also like to thank my parents for their encouragement throughout my academic endeavors, and my colleagues Madeline Camp and Anna Getler for their tenacious friendship on all accounts, for the duration of this Masters' program and beyond.

SEX AND ANCESTRY ESTIMATION USING COMPUTED TOMOGRAPHY: A COMPARISON OF THE RELIABILITY OF DIGITAL VERSUS PHYSICAL DATA COLLECTION

ELENA JANOWIAK

ABSTRACT

Sex and ancestry are most commonly estimated by anthropologists using the skull. Typically, measurements and observations are taken on the skull itself, but for the purpose of convenience, computed tomography (CT) scans are increasingly used in place of skulls in research and forensic casework. Researchers work under the assumption that the dry skull-to-CT scan ratio is one-to-one; however, research on the accuracy of CT scans is sparse. In this study, eight skulls from the Boston University Donated Skeletal Collection were scored for sex and ancestral morphological traits following Buikstra and Ubelaker (1994) and Hefner and Ousley (2014), and measured using standard cranial measurements according to Langley et al. (2016). CT scans were then taken of the eight skulls and the same morphological observations and measurements were taken using the RadiAnt 5.5.1 CT viewer. Additionally, the measurements of each skull and scan were entered into FORDISC 3.1, a software program that provides discriminant functions for the processes of sex and ancestry estimation. The measurements for each dry skull-CT scan pairing were then analyzed for variance and mean differences. The results of the morphological and metric analyses indicate that the majority of the data gathered from *dry skulls did not vary significantly from the measurements taken on the CT scans. The morphological sex estimation resulted in the same estimation for each skull-to-CT scan pairing; however, the morphological ancestry estimation results indicated that skeletal information lost in CT scans can make full visualization and therefore assessment of the facial region difficult. The FORDISC 3.1 results generally support the indication that there is not a significant difference between skull and CT scan measurements, with consistent sex estimation results for each dry skull-to-CT scan pairing and consistent ancestry estimation results for the majority of the pairings. However, the sex and ancestry estimations were not always accurate considering the true ancestral backgrounds of the individuals. Based on these outcomes, it is evident that CT scans can be used to obtain reliable morphological assessments and measurements of a skull, which can then be used to estimate sex using FORDISC 3.1. However, to ensure accuracy of the sex and ancestry estimations, other methods should be used in conjunction with FORDISC 3.1.*

TABLE OF CONTENTS

ACKNOWLEDGEMENTS iv

ABSTRACT v

TABLE OF CONTENTS vii

LIST OF TABLES ix

LIST OF FIGURES x

LIST OF ABBREVIATIONS xiii

Chapter I: INTRODUCTION 1

1.1: Background 1

1.2: Cranial Morphological Sex and Ancestry Estimation 2

1.3: Cranial Metric Sex and Ancestry Estimation 3

1.4: Purpose 4

Chapter II: PREVIOUS RESEARCH 7

2.1: History 7

2.2: Morphological Methods 10

2.3: Metric Methods 18

2.4: Applications of CT Scanning Technology 23

2.5: Conclusions 35

Chapter III: MATERIALS AND METHODS 36

3.1: Materials 36

3.2: CT Scans 45

3.3: Morphological Methods 52

3.4: Metric Methods 58

3.5: Statistical Analysis 64

Chapter IV: RESULTS 66

4.1: Morphological Sex Estimation Results 66

4.2: Morphological Ancestry Estimation Results 70

4.3: Statistical Analysis of Measurements 75

4.4: FORDISC 3.1 Sex and Ancestry Estimation 79

4.5: Conclusion 82

Chapter V: DISCUSSION 84

5.1: Morphological Analysis 84

5.2: Measurements 85

5.3: FORDISC 3.1 Analysis 87

5.4: Comparison of Morphological and Metric Methods 89

5.5: Limitations 90

Chapter VI: CONCLUSIONS 93

6.1: Viability of CT Scans 93

6.2: Implications of the Current Research 95

6.3: Further Directions and Recommendations 97

REFERENCES 99

CURRICULUM VITAE 107

LIST OF TABLES

Table	Title	Page
3.1	Skull name designations for the purpose of this study and actual sex, ancestry, and age of donor individuals.	36
3.2	Cranial landmarks. Adapted from Langley *et al.* (2016).	60
3.3	Measurements used in FORDISC analysis. Adapted from Langley *et al.* (2016).	63
4.1	Logistic discriminant analysis equations for sex estimation from Walker (2008: 47).	68
4.2	Morphological sex estimation using discriminant function equations from Walker (2008).	69
4.3	Dry skull measurements.	76
4.4	CT scan measurements.	76
4.5	One-way ANOVA results for each measurement.	77
4.6	Minimum, maximum, and mean deviations for each measurement.	78
4.7	FORDISC 3.1 statistics for sex estimation.	79
4.8	FORDISC 3.1 statistics for ancestry estimation.	81

LIST OF FIGURES

Figure	Title	Page
2.1	FORDISC 3.1 data entry page.	21
2.2	Maxillary (top) and mandibular (bottom) dentition of Skull 8. Note the distortion caused by metal dental restorations in the CT scans.	25
3.1	Skull 1. Anterior view, left lateral view, and superior view of mandible.	37
3.2	Skull 2. Anterior view, left lateral view, and superior view of mandible.	38
3.3	Skull 3. Anterior view, left lateral view, and superior view of mandible.	39
3.4	Skull 4. Anterior view, left lateral view, and superior view of mandible.	40
3.5	Skull 5. Anterior view, left lateral view, and superior view of mandible.	41
3.6	Skull 6. Anterior view, left lateral view, and superior view of mandible.	42
3.7	Skull 7. Anterior view, left lateral view, and superior view of mandible.	43
3.8	Skull 8. Anterior view, left lateral view, and superior view of mandible.	44
3.9	CT scan of skull 1. Left lateral and anterior views.	46
3.10	CT scan of skull 2. Left lateral and anterior views.	46
3.11	CT scan of skull 3. Left lateral and anterior views.	47
3.12	CT scan of skull 4. Left lateral and anterior views.	47
3.13	CT scan of skull 5. Left lateral and anterior views.	48
3.14	CT scan of skull 6. Left lateral and anterior views.	48
3.15	CT scan of skull 7. Left lateral and anterior views.	49
3.16	CT scan of skull 8. Left lateral and anterior views.	49

3.17	Skulls 6 (left) and 8 (right), superior view. Note the poorly defined coronal, sagittal, and occipital sutures.	51
3.18	Cranial morphological character states from Buikstra and Ubelaker (1994:20).	53
3.19	Anterior nasal spine character states from Hefner (2009:987).	55
3.20	Inferior nasal aperture character states from Hefner (2009:988).	55
3.21	Interorbital breadth character states from Hefner (2009:988).	56
3.22	Nasal aperture width character states from Hefner (2009:989).	56
3.23	Nasal bone structure from Hefner (2009:989).	56
3.24	Post-bregmatic depression character states from Hefner (2009:990).	57
3.25	OSSA scoring table from Hefner and Ousley (2014:4).	58
3.26	FORDISC 3.1 data entry page.	62
4.1	Scoring results following Walker (2008) and Buikstra and Ubelaker (1994).	67
4.2	OSSA scores for Skull 1 and CT Scan 1 using chart in Hefner and Ousley (2014:4).	70
4.3	OSSA scores for Skull 2 and CT Scan 2 using chart in Hefner and Ousley (2014:4).	71
4.4	OSSA scores for Skull 3 and CT Scan 3 using chart in Hefner and Ousley (2014:4).	71
4.5	OSSA scores for Skull 4 and CT Scan 4 using chart in Hefner and Ousley (2014:4).	72
4.6	OSSA scores for Skull 5 and CT Scan 5 using chart in Hefner and Ousley (2014:4).	72
4.7	OSSA scores for Skull 6 and CT Scan 6 using chart in Hefner and Ousley (2014:4).	73

4.8	OSSA scores for Skull 7 and CT Scan 7 using chart in Hefner and Ousley (2014:4).	73
4.9	OSSA scores for Skull 8 and CT Scan 8 using chart in Hefner and Ousley (2014:4).	74

LIST OF ABBREVIATIONS

ANOVA: Analysis of variance

ASB: biasterionic breadth

AUB: biauricular breadth

BBH: basion-bregma height

BNL: basion-nasion length

BPL: basion-prostheon length

CDL: bicondylar breadth

CT: Computed tomography

DKB: interorbital breadth

EKB: biorbital breadth

FOB: foramen magnum breadth

FOL: foramen magnum length

FRC: frontal chord

GNI: chin height

GOG: bigonial breadth

GOL: maximum cranial length

HMF: height at mental foramen

MAB: palate breadth

MAL: palate length

MAN: mandibular angle

MDH: mastoid height

MLN: mandibular length

MOW: midorbital width

NLB: nasal breadth

NLH: nasal height

OBB: orbital breadth

OBH: orbital height

OCC: occipital chord

PAC: parietal chord

TMF: breadth at mental foramen

UFBR: upper facial breadth

UFHT: upper facial height

WFB: minimum frontal breadth

WRB: minimum ramus breadth

XCB: maximum cranial breadth

XRH: maximum ramus height

ZMB: zygomaxillary breadth

ZYB: bizygomatic breadth

3D: three-dimensional

Chapter I: INTRODUCTION

1.1 Background

In the fields of forensic and biological anthropology, it is not always possible or practical to transport human remains in order for them to be examined elsewhere. Further, capturing the details needed for proper analysis in a portable format can be a challenge. When access to the remains themselves is not an option, researchers are limited to photographs or radiographs of the remains in question. Even when a scale is provided in the image, metric analysis often cannot be accurately conducted using images alone.

A more effective option for reproduction and distribution of skeletal remains is radiological scans, such as x-rays and computed tomography (CT) scans. CT scans create a three-dimensional digital model of the bones (and other structures) to be studied. They are most commonly used in the medical field and are regarded as very accurate when taken from living and deceased subjects, but the technology is made specifically to be used on subjects with soft tissue covering the bone. Therefore, the resolution of scans taken of bone-only study materials may not have the same degree of accuracy as those taken in medical situations.

In addition to being useful in situations where only bone is present, CT scans can allow for an extensive forensic anthropological analysis of skeletal remains when the subject is still fleshed. Through medical technology, the individual can be scanned so that the bones may be accessed in three dimensions without the need to macerate the individual. This way, processes of analysis in forensic anthropology and forensic pathology can be carried out at the same time, expediting the process of information gathering in forensic cases. Additionally, since current skeletal collections are limited in regards to demographics, the use of CT scans holds important research potential. CT scans allow researchers access to skeletal data for increasingly diverse populations without the need for physical skeletal materials, which are typically restricted in terms of age and ancestral background.

1.2 Cranial Morphological Sex and Ancestry Estimation

This study focused on cranial sex and ancestry estimation techniques and whether they can be effectively used with CT scans of skulls. Morphological traits for sex and ancestry were scored following Walker (2008) and Hefner and Ousley (2014), respectively. Walker (2008) includes five morphological traits for scoring sex using the cranium based on a scoring system presented by Buikstra and Ubelaker (1994). The scoring system instructs the observer to rate cranial traits on a scale from one to five based on robusticity, with one being the most gracile and five being the most robust. These ordinal scores are then entered into binary logistic discriminant analysis equations, which output probable sex.

Hefner and Ousley (2014) created a system of scoring six cranial morphological traits to differentiate ancestry between Black and White individuals, called the optimized summed scored attributes (OSSA) method. Different states for each trait are scored, and each has unique criteria for scoring. These state scores each correspond to a different OSSA score, which are binarized; either zero or one. The OSSA scores for each trait are then added up, and the overall score corresponds to the most likely ancestral group and strength of correlation (given the individual is of African- or European- derived ancestry). The OSSA method is consolidated into a chart, which is included for each skull and cranial CT scan scored.

1.3 Cranial Metric Sex and Ancestry Estimation

In addition to morphological methods, this study assessed the ability to obtain accurate measurements from cranial CT scans. Measurements on the dry skulls were taken according to standard practice using Langley *et al.* (2016). These measurement methods were then adapted to use within 3D-rendered CT scan viewing software. To determine if there were significant differences in measurement between the skulls and CT scans, one-way analysis of variance (ANOVA) tests were run on each individual measurement. In previous research, there have been many studies which have compared the accuracy of measurements taken from dry bone to those taken from CT scans (Colman *et al.* 2019; Stull *et al.* 2014; Zech *et al.* 2012); however, this particular study paired the measurements with a common forensic anthropological application by entering the measurements into FORDISC and assessing the resultant sex and ancestry estimations.

FORDISC 3.1 is a program created by Jantz and Ousley (2005) that automates the process of estimating sex and ancestry using standardized skeletal measurements in conjunction with linear discriminant function analysis. While an effective tool for assessing sex and ancestry, there are limitations in assessing ancestry as the groups included in FORDISC are limited to White males, White females, Black males, Black females, Hispanic males, Hispanic females, American Indian males, American Indian females, Japanese males, Japanese females, Guatemalan males, Vietnamese males, and Chinese males. However, the forensic database within FORDISC (which is the dataset used for the analysis in this study) includes data of over 3,000 individuals from eight ancestral groups (Jantz and Ousley 2005). In order to obtain sex and ancestry estimates from FORDISC, the measurements from the skull are entered into the system and the program groups the measurements into the closest sex and ancestral fit.

1.4 Purpose

The main goal of this study is to assess the validity of morphological and metric data gathered from CT scans of skulls versus the same data gathered from the actual dry skulls. This includes comparison of morphological data for sex and ancestry estimation, as well as testing the consistency of FORDISC 3.1 analysis between dry skull-derived measurements and CT scan-derived measurements of the same skulls. In addition to the examination of sex and ancestry estimations, the measurements themselves are compared for variance to determine if CT scan-derived measurements can be used in place of dry skull-derived measurements. The results will provide data confirming the efficacy of using CT scans in place of real skulls for analysis in biological anthropology and medical research, or cautioning against the use of CT scans in analysis due to disparities in measurements or morphological trait appearances.

This study contributes to the existing literature validating the use of CT scan-derived data in the place of traditional forensic anthropological examination. Data gathered using CT scans is important in that it allows for the collection of osteological data on a very modern (e.g., living) sample of individuals, thereby helping to mitigate the issues around the lack of diversity represented in the common skeletal collections used for research. In addition to the ostensible benefit to research samples, CT scan analysis in a forensic setting allows osteological data to be collected without the need to macerate the body. Not only does this save time, but it also provides an avenue with which traditional autopsy may be possibly bypassed in the future, accommodating for religious beliefs that oppose autopsy (Cressey 2010). In both the contexts of research and forensic casework, CT scan data will likely be the "way of the future" so to speak for advancing skeletal biology methods.

The following chapter (II) of this study provides a discussion of previous research related to the question at hand, including the development of the practices of sex and ancestry estimation in biological anthropology, modern methods of sex and ancestry estimation, and applications of CT scanning technology to medical, paleoanthropological, and forensic research and casework. The third chapter contains a description of the materials and methods used to conduct this study. The fourth chapter includes the results of the morphological and metric analyses of the dry skulls and CT scans, including sex and ancestry estimation using morphological methods and FORDISC 3.1 findings. The fifth chapter includes a discussion of the study overall, and finally, the sixth chapter includes concluding thoughts and recommendations.

In conclusion, the purpose of this study is to evaluate the hypothesis that metric and morphological data gathered using cranial CT scans is equally as accurate and useful as metric and morphological data gathered using forensic anthropological methods on dry skulls. This includes data in the form of standard cranial measurements and sex and ancestry estimation using methods published by Walker (2008), Hefner and Ousley (2014), and FORDISC (Jantz and Ousley 2005).

Chapter II: PREVIOUS RESEARCH

2.1 History

The utility of using morphological and metric data from the human skull to estimate the ancestry of the deceased individual has been extensively studied. Early studies used morphological traits to sort skulls by shape, with five major categories: Australoid, Caucasoid, Congoid, Mongoloid, and Capoid (Relethford 2010). These five categories are now typically grouped into three categories: Caucasoid, Mongoloid, and Negroid, which have been used to categorize remains for years (Bass 2005; Rhine 1990). While the distinctions between the morphological traits of the skulls of different ancestral groups are based in genetics and population history, the wording, methods, and applications of this typological style of research have become antiquated. Estimation of ancestry has come a long way since its scientific inception. Most recently, methodologies for establishing ancestry are much less ignoble than they were in the past, as these methods aid forensic anthropologists in building of a biological profile for unidentified individuals to aid in identification efforts.

In the eighteenth and nineteenth centuries, the scientific Enlightenment period led to an interest in human origins and variation. Early scholars began linking traits between apes and humans and developing a typological approach for characterizing "race." Some scientists believed that the "races" of humans represented separate species, whereas others recognized that all humans are the same species (Little and Sussman 2010). Even these "modern" minds had significant bias, however, with some subscribing to the belief that God had created the races separately in a hierarchical fashion, in which some races were inferior to others, called “polygenism.” On the other hand, “monogenism” was the belief that humans shared a single origin (Little and Sussman 2010). This belief was not less racist, however, because it included the opinion that races other than Caucasian had degenerated (Stocking 1988).

In the early- to mid-twentieth century, the conversations and study of race continued, but also directly contributed to racially-driven atrocities in the form of the eugenics movement. A change in attitude came amid the changing sociocultural climate following the criminal atrocities committed during World War II and issues brought to the forefront during the civil rights movement. The 1950s and 1960s was a period of change in the field of biological anthropology, particularly regarding attitudes on ancestral variation. Biological anthropology began the transition from viewing human variation through classification to understanding the evolutionary basis of these variations (Relethford 2010; Stini 2010; Washburn 1951). It was a contentious time period; many anthropologists began rejecting typological views on “race,” while others disagreed and held on to their racist beliefs that ancestral groups are inherently different. There was a shift in scientific dialogue from thinking of human variation as distinct races to viewing them as mutable and dynamic populations (Little and Sussman 2010).

A key turning point in physical anthropology was prompted by Washburn’s (1951) conception of the “New Physical Anthropology,” which revolutionized how the field views human variation. The mindset was turned away from typological classification to genetically-driven studies of variation between populations due to geographic distance and natural selection processes (Washburn 1951). The “New

Physical Anthropology" also accentuated the need to apply the scientific method to studies of human variation, thus transforming physical anthropology from a science of speculative observation to a legitimate branch of biological science (Stini 2010). However, by this time period the concept of race and a racial hierarchy of supremacy was already prevalent in the global sociocultural mind, where it still causes issues today. Despite the issues, when anthropologists are working with law enforcement, medical examiners, and other investigative agencies, it is standard practice that identification efforts call for an individual to be sorted into social "race" categories.

This interest in human variation, however biased, led to the study of human origins, anthropometry, craniometry, anatomy, osteology, and morphological traits, paving the way for understanding of human variation in modern biological anthropology. Today, the concept of biological race as a sociocultural construct is widely accepted in the modern scientific community (Caspari 2010; Stini 2010). The understanding of human genetic variation and its morphological manifestations is still extensively studied by biological anthropologists, significantly for the purpose of estimating ancestral background using skeletal measurements and morphology (Bass 2005; Brues 1990; Gill 1998; Hauser and De Stefano 1989; Hefner and Ousley 2014; Hefner 2009; Krogman and İşcan1986; Rhine 1990). Other information included in skeletal biological profile studies, including sex, stature, and age, also can be counted as products of biological anthropology's contentious past.

Today, to be used as evidence in a court of law, all methodologies and techniques used in forensic science must meet the requirements of either the standard of *Frye v.*

United States (293 F. 1013 (D.C. Cir 1923)), which asserts that the science must be sufficiently established to have gained general acceptance in the particular field in which it belongs, or, more commonly, the standards established by *Daubert v. Merrell Dow Pharmaceuticals* (509 U.S. 579 (1993)), which state that science used in a court of law must: 1) be testable and tested through the scientific method; 2) be subject to peer review; 3) be based on established standards; 4) have a known error rate; and 5) be widely accepted by the scientific community to which it belongs. *Daubert* is used in most states and in federal courts in the United States. Because of these standards, it is of the utmost importance that applications of forensic science be tested.

2.2 Morphological Methods

The simplest, longest-practiced method of estimating the sex and ancestry of an individual from a skull is visually, using morphological variation. Early manifestations of this approach lacked statistics, were based in observer experience, and were typological. These morphological methods of estimating ancestry are often preferred over metric methods for their practicality since they do not require equipment. However, there is often poor inter-observer agreement and wide variability in traits results from intermixing of ancestral groups and idiosyncratic variation. Overall, the mid-facial region, palate shape, palatine suture, and mastoid form are thought to be the most useful areas in estimation of ancestry (Gill 1998; Rhine 1990). Any one trait may be too ambiguous to determine ancestry, but it is combinations of distinct traits that will provide the final estimation.

Morphological traits that are commonly used to assess ancestry include interorbital breadth (Bass 2005; Hefner 2009; Rhine 1990), nasal aperture width (Bass 2005; Hefner 2009; Rhine 1990), post-bregmatic depression (Bass 2005; Hefner 2009; Rhine 1990; Krogman and İşcan1986), anterior nasal spine (Hefner 2009; Rhine 1990), inferior nasal aperture (Hefner 2009; Rhine 1990; Krogman and İşcan1986), malar tubercle (Hefner 2009; Rhine 1990; Hauser and De Stefano 1989), nasal bone contour (Hefner 2009; Rhine 1990), nasal overgrowth (Hefner 2009; Rhine 1990), supranasal suture (Hefner 2009; Hauser and De Stefano 1989), transverse palatine suture (Hefner 2009; Rhine 1990; Hauser and De Stefano 1989), and zygomaticomaxillary suture (Hefner 2009; Rhine 1990; Hauser and De Stefano 1989), among others. Many publications in use today for morphological ancestry estimation only distinguish between three major groups: Caucasoid, Negroid, and Mongoloid (Bass 2005; Rhine 1990). Although the wording has become outdated and insensitive, the distinctions drawn between these groups early on have since been researched and largely confirmed to be scientifically relevant.

Although they have proven useful, visual methods can introduce errors related to subjectivity of the assessors, and observations in earlier literature often lack diversity and statistical backing, with findings relying heavily on observer experience. Differences between the bones of individuals of different ancestral backgrounds have long been noted, but differences were not studied and scientifically observed using multivariate statistical analysis until later. It has been found that although scoring morphological traits as “present” or “absent” causes loss of specific information, it also decreases subjectivity and therefore the present/absent system of observation may decrease inter-observer error. Another shortcoming prevalent in ancestral estimation is lack of diversity in research. Rarer ancestral groups may not have high enough sample sizes or may not have ever been studied at all, either due to lack of sample for study or lack of researcher interest. Even given these limitations, many studies have been conducted that validate morphological methods of ancestry estimation, not only by mere association but with robust statistics and inter-observer success.

One such study is that of Hefner and Ousley (2014), in which six cranial morphological traits with robust statistical validation for ancestry estimation were selected and used to create a scoring system. This system, called OSSA, can be used to estimate whether an individual is of Black or White ancestry. Traits used in OSSA analysis are described the anterior nasal spine, inferior nasal aperture, interorbital breadth, nasal aperture width, nasal bone structure, and post-bregmatic depression, each with a unique set of character states (described in Hefner 2009) which correspond to an OSSA score of either one (common in American Whites) or zero (common in American Blacks). These scores are then summed, and the summed OSSA score corresponds to an ancestry estimation of Black or White. This system operates under the consideration that individual morphological ancestral traits are expressed in a composite fashion rather than all together as expressed in illustrations by Bass (2005) and Rhine (1990). Whereas Rhine (1990) and Bass (2005) merely make observations of trends in trait expression for different ancestral groups, Hefner and Ousley (2014) provide a more statistically robust method of classification.

Although a generally accurate method, there are a few significant problems with Hefner and Ousley's (2014) OSSA method. One problem is that it is only useful for classifying remains into two ancestral varieties: American Black and American White. Although these populations are often forensically relevant, this greatly limits the utility of the method, as well as failing to account for trait overlap between these two populations. Also, the method weighs all traits equally, when in reality each trait may be variably efficient at predicting ancestral background, and the results do not provide any statistical probabilities associated with the estimation. Furthermore, all six traits must be present for the method to work.

In addition to the estimation of ancestry, the skeleton can be used to estimate the sex of a deceased individual. While sex differences are often readily apparent in the flesh, distinctions in shape and size are also detectable in the skeleton to the trained professional, particularly in the pelvic region and the skull. For morphological sex estimation, the pelvis is widely accepted as the skeletal region that manifests the most sexually dimorphic features that provide the most accurate estimations, followed by the skull. Like many other animal species, adult humans are sexually dimorphic, although much less so in comparison to other non-human primates. In short, this means that biological males tend to be larger with more robust muscle attachments and sharper features, while biological females tend to have smaller features and muscular attachments with more rounded features. Morphologically and metrically, males can be up to 20% larger than females (White *et al*. 2012), although the actual dimensions and morphological expression can overlap near the middle of the spectrum. This overlap can be caused by human variation and ancestry, which can confound sex estimation, as some ancestral groups have gracile males and some have robust females. For example, morphological sex estimation methods developed on European- or African-derived ancestral populations (such as those by Garvin *et al.* 2014 and Walker 2008) tend to perform poorly on individuals of Asian descent due to this group's decreased sexual dimorphism (Tallman 2019).

There are fewer confounding variables in sex estimation than there are in ancestry estimation. In the typical forensic biological profile, sex is limited to the binary male/female distinction (although in actuality, biological sex is much more nuanced), whereas ancestry consists of innumerable groups that frequently change and meld together. Even given the relative simplicity of sex estimation, it must be noted that when identifying an individual, biological sex must not be confused with gender. Biological sex is a label assigned based upon hormones, chromosomes, and genitalia, whereas gender is a manifestation of social expectations, behavioral characteristics, intrinsic personal thoughts, and self-expression experienced as an individual, which may or may not coincide with biological sex. Typical research issues apply to sex estimation as well, such as inter-observer error and lack of study on sexual dimorphism in various ancestral groups.

Cranial sex estimation is commonly conducted using Walker's (2008) logistic discriminant analysis equations for predicting sex based off of Buikstra and Ubelaker's (1994) cranial scoring system. Buikstra and Ubelaker's (1994) scoring system is used to score the physical appearances of the nuchal crest, mastoid process, supraorbital margin, glabella, and mental eminence based on a 6-category numbering system that goes from gracile to robust, with 0 being undetermined, 1 being female, 2 being probable female, 3 being ambiguous, 4 being probable male, and 5 being male.

Walker's (2008) scoring system, like Buikstra and Ubelaker's (1994), is used to score the physical appearances of the nuchal crest, mastoid process, supraorbital margin, glabella, and mental eminence on a scale from 1-5 (gracile to robust). Unlike Buikstra and Ubelaker's (1994) scoring system, however, Walker's lacks the associated male and female descriptors and instead uses the scores entered into logistic discriminant analysis equations to estimate the sex of the individual. While highly accurate within American/English White and Native American populations, these equations are not designed for use with other populations. However, for the purposes of the current research presented in this study, in which all individuals are of European-derived ancestry, these equations work.

Garvin *et al.* (2014) conducted a validation study of Walker's (2008) scoring system, assessing the effects of population, age, and body size on the estimation of sex by evaluating correlations between these variables and Walker's trait scores. It was found that population had a significant effect on trait scores, whereas neither age nor body size had significant influence on the expression of traits. The traits that were found to be most reliable were glabella and mastoid processes, and the nuchal crest was the least reliable. Overall, Garvin *et al.* (2014) recommend that researchers and forensic caseworkers use population-specific discriminant functions when estimating sex of an unknown individual. One such example of a population-specific set of logistic regression equations was developed for Asian populations by Tallman (2019). This study improved the application of Walker's (2008) method for use in diverse Asian-derived groups, including Japanese, Thai, and Filipino populations.

Morphometrically, the shape of the forehead of the skull (nasion to glabella; see Table 3.2 for details on craniofacial landmarks) has been found to also be sexually dimorphic in a study that used Elliptical Fourier Analysis of the forehead, the nasion to bregma contour, supraorbital ridge, and orbital borders (Inoue 1990). It was observed that males tend to have more developed supraorbital ridges and more sloping foreheads, and females have less pronounced supraorbital ridges and higher more rounded foreheads. Shape-based methods of sex estimation are claimed by Inoue (1990) to be more accurate than distance-based quantitative methods.

Preferred over the cranium, the pelvic girdle is regarded as the most effective and reliable skeletal element for morphological sex estimation due to morphological differences related to child-bearing. On the os coxae, character states of the greater sciatic notch (Walker 2005) and pubis region (Phenice 1969; Klales *et al.* 2012) are reliable indicators of sex. Phenice (1969) observed sexual dimorphism of the ventral arc, subpubic contour, and medial aspect of the ischiopubic ramus on the pubis. These observations that were later modified by Klales *et al.* (2012) to include an ordinally-scaled range of expressions from most feminine (1) to most masculine (5). A binary logistic regression equation was then developed, much like Walker's (2008) work with Buikstra and Ubelaker's (1994) cranial traits, with highly accurate results and low intra- and inter-observer errors. Contrary to findings by Garvin *et al.* (2014) regarding the effects of population on cranial sex estimation, Klales *et al.* (2012) found that ancestry had no effect on the accuracy of their discriminant function.

A newly developed way to estimate sex using morphological traits of the skull and pelvis, MorphoPASSE (Morphological pelvis and skull sex estimation program) is an automated system similar to Jantz and Ousley's (2005) FORDISC (see next section 2.3), which allows users to estimate sex of an unknown individual using ordinal scores from Walker (2008) and Klales *et al.* (2012). The comparative database includes samples of contemporary, historic, proto-historic, and pre-historic individuals from Asian, Black, Hispanic, Native American, White, and Nubian ancestral backgrounds. After the scores have been entered, they are automatically run through either binary logistic regression equations or analyzed with random forest modeling, at the choice of the user. Random forest modeling is a machine leaning algorithm which produces an average prediction based on a randomly generated "forest" of decision trees. The random forest modeling option allows for more flexibility, as it can be used for analysis even with information missing. The system outputs a case prediction for the individual including probabilities, as well as weighted importance of each trait used in the analysis, as well as data on error rates based on the random forest modeling. MorphoPASSE will likely become widely used in the future due to its extensive and diverse database, accessibility, and straightforward operation.

Postcranially, aside from the pelvis, the distal humerus has been observed to be sexually dimorphic as well (Vance *et al.* 2011; Rogers 1999). Morphological traits such as the medial epicondylar angle, olecranon fossa shape, trochlear extension, and trochlear constriction have been found to be significant in the estimation of sex. Tallman and Blanton (2020) modified Vance *et al.* (2011) and Rogers' (1999) observations of sexual variations in the distal humerus, altering them to include a range of five character states for each trait that describe their morphology rather than simply a scale of "feminine" to "masculine." The validity of this scoring method was confirmed on a Thai population using composite scoring, binary probit regression, binary logistic regression, and univariate analysis

2.3 Metric Methods

In addition to morphological methods of estimating ancestry, metric methods can also be used. These methods involve measuring the distance between certain features and landmarks on the skull and using these measurements to statistically estimate which ancestral group the given individual is closest to using equations that have been established use large known data sets. These methods are considered more objective and reliable than morphological methods, but the reliability of the estimation depends on the accuracy of the assessor, the accuracy of the tools being used to measure, and the correct application of statistical analysis.

The study of metric methods of ancestry estimation came after morphological methods. In earlier studies, it was found that a larger number of variables does not necessarily make ancestry and sex estimation more accurate, but it is better to have specific reliable variables with high discriminatory power (Johnson *et al.* 1990). Metric sex and ancestry estimation work very similarly, in that measurements from bones are taken and then any number of these measurement variables are entered into discriminant function equations that output probable sex. It has been found that the best metric variables used for ancestry estimation are not those that are best for sex estimation (Johnson *et al.* 1990). Similar to morphological sex estimation, in metric analysis the pelvis and skull tend to be the prime areas of interest. Historically, it has been generally accepted that the skull performs well in sex estimation, although postcranial elements have been found to outperform cranial metric sex estimation methods (Spradley and Jantz 2011). Population-specific and population-independent binary logistic regression models based on metric variables have been developed for the humerus (Attia and Abulnoor 2020; Mall *et al*. 2001; Moore *et al*. 2016; Spradley and Jantz 2011; Patterson and Tallman 2019), radius (Mall *et al*. 2001; Spradley and Jantz 2011; Patterson and Tallman 2019), ulna (Mall *et al*. 2001; Moore *et al*. 2016; Spradley and Jantz 2011; Patterson and Tallman 2019), femur (Attia and Abulnoor 2019; Curate *et al.* 2016; Carvallo and Retamal 2020; Spradley and Jantz 2011; Patterson and Tallman 2019), scapula (Moore *et al*. 2016; Spradley and Jantz 2011; Patterson and Tallman 2019), clavicle (Moore *et al*. 2016; Spradley and Jantz 2011; Patterson and Tallman 2019) and the sternum (Franklin *et al.* 2012), to name a few, with classification rates performing as well as or better than those developed on crania.

To facilitate the ability to efficiently estimate metric sex and ancestry of skeletal remains using osteometric measurements, FORDISC was developed by Jantz and Ousley (2005). FORDISC uses measurements from a large group of individuals of known sex and ancestry to establish a baseline of statistical trends in measurements that can then be used to estimate sex and ancestry using measurements taken from the remains of unidentified individuals using customized discriminant function equations. It was developed to expedite and objectify the process of metrically estimating sex, ancestry, and stature. The volume of diverse individuals comprising the FORDISC databases makes estimation of these aspects of the biological profile more expeditious than seeking population-specific equations for estimation of sex, ancestry, and stature in the extensive scientific literature that exists on these topics. Populations included are White males, White females, Black males, Black females, Hispanic males, Hispanic females, American Indian males, American Indian females, Japanese males, Japanese females, Guatemalan males, Vietnamese males, and Chinese males.

When the user enters metric data into the FORDISC opening screen (Figure 2.1) and clicks “process,” the data is automatically run through the applicable discriminant function equations and outputs a list of possible classifications for the individual based on the measurement data (Jantz and Ousley 2005). This list includes multiple ancestry/sex combinations and statistics for Distance from, Posterior, Type F, Type Chi, and Type R probabilities for each, along with an overall recommended classification if the statistics suggest one group strongly. The “Distance from” column tells the Mahalanobis distance the remains are from each group, ordered from least distant to most distant. The “posterior probability” column tells the probability the skull belongs to each group included under the assumption it must belong to one of the groups, and the rest of the columns are typicality probabilities that do not assume the skull belongs to an included group. The resulting distance and probabilities are the responsibility of the researcher to interpret, making the process, as all science is, vulnerable to bias. Although not infallible, it is a very useful resource.

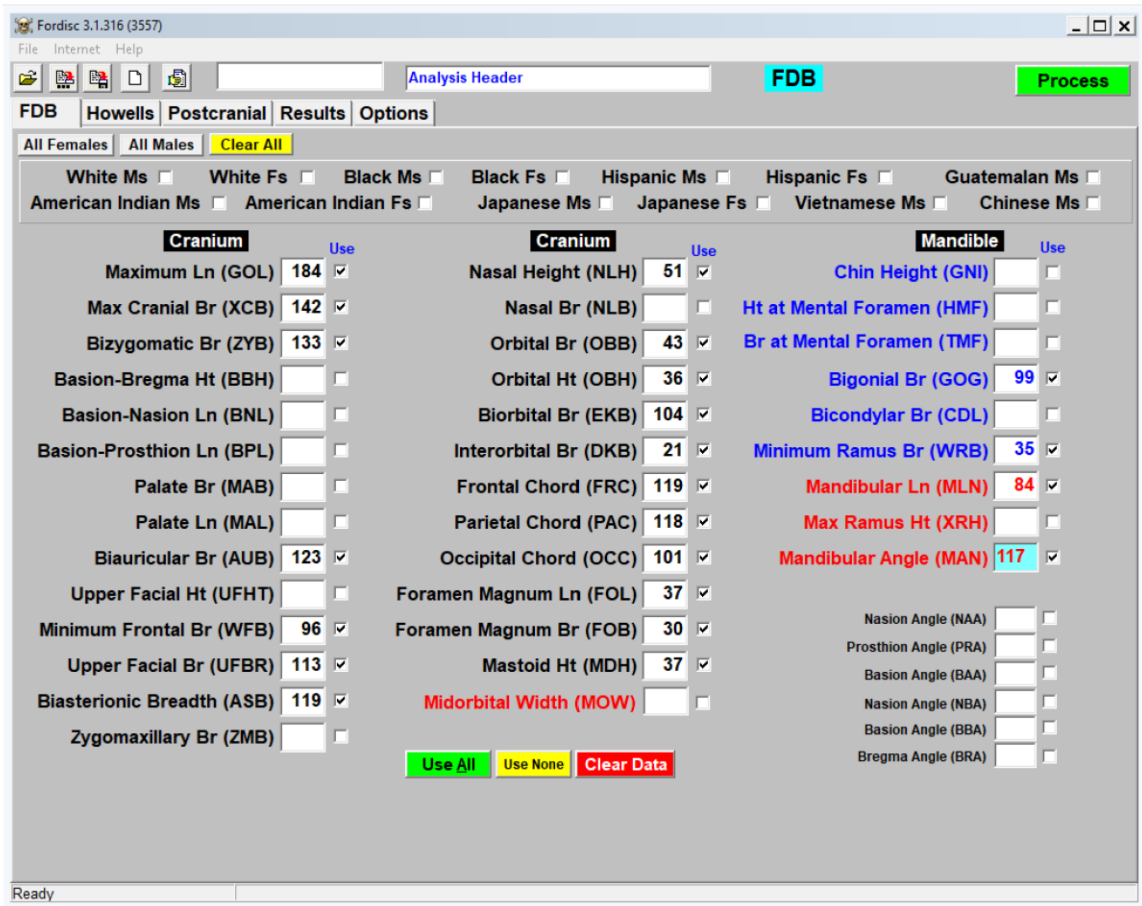

Figure 2.1. FORDISC 3.1 data entry page.

Several studies testing the accuracy of FORDISC analysis have been conducted, and often with concerning results. A study using FORDISC 3.0 (the previous edition of FORDISC) by Guyomarc'h and Bruzek (2011) tested the accuracy and reliability of sex estimation using the program on French and Thai subsamples, and they found that the sex and ancestry of the Thai sub-sample was not predicted accurately and the French subsample had better accuracy rates, but neither were very good. Misclassification of individuals of Hispanic ancestry as Japanese is also a noted issue with FORDISC. A study by Dudzik and Jantz (2016) explored this phenomenon, and found that Hispanic individuals are also often misclassified as White or Native American. Comparisons of the morphologies of Hispanic and Japanese samples yielded a smaller than expected distance, explaining the high instance of misclassification. The proposed explanation for these classification issues are shared evolutionary histories between Hispanic populations and Japanese, White, and Native American populations. Another study by Elliott and Collard (2009) tested FORDISC classification of a large sample of 200 specimens of known ancestry, and found that only 1% of their sample was classified correctly.

Although automatic and straightforward, FORDISC analysis is clearly not always accurate and can be altered in many ways. There are multiple options within the program to alter which measurements are taken into consideration (note the check boxes next to each measurement in Figure 2.1), and researchers can easily intentionally or unintentionally alter the results to fit their bias. Despite the studies by Guyomarc'h and Bruzek (2011), Elliott and Collard (2009), and Dudzik and Jantz (2016) yielding less than satisfactory results, among other limitations, FORDISC is still widely accepted and used by forensic anthropologists to estimate sex and ancestry of unknown individuals. Given its flaws, however, this analysis should be combined with additional methods of sex and ancestry estimation to support the results.

In the pursuit of the highest possible level of objectivity, commonly used metric methods are evolving into higher-tech methods of sex and ancestry estimation, involving machine learning. This is accomplished by feeding numerous scans of known skulls into a computer program, which "teaches" the software to recognize trends in 3D morphometric variables (Bertsatos *et al.* 2019; Bewes *et al.* 2019). This way, a skull from an unknown individual may be scanned and simply put into the program which will estimate the individual's ancestry and sex without the need for an assessor taking physical measurements (Bertsatos *et al.* 2019). However, given the innumerable ancestral backgrounds and the broad scope of human variation worldwide, there is much room for ambiguity within known groups and a dearth of data for the rest of the groups. In fact, morphometric sex estimation through machine-learning technology was found to be even more accurate than ancestry estimation in a study by Bertsatos *et al.* (2019). This same study confirms the evidence found by Johnson *et al.* (1990) that using fewer craniometric landmarks with stronger associative power yield better results than if many landmarks with weaker discriminative power are used. Machine-learning based sex estimation is less subjective than other methods of sex estimation such as morphological or metric methods carried out by individual researchers due to automation. Artificial intelligence sex estimation has been found to be up to 95% accurate (Bewes *et al.* 2019).

2.4 Applications of CT Scanning Technology

Biomedical imaging, including CT scanning, is used commonly in medical and forensic research, medical practice, and forensic investigation. These digitally rendered images allow researchers to view internal structures of the human body while the individual is intact as well as provide visual data on bone or tissue in a format that is easily transported and distributed. Once the body has been scanned, the demanding task of physically transporting the human remains is rendered obsolete. Transporting human remains, especially while the soft tissue is still present, can be a complicated, sensitive, or even impossible endeavor. Because of this, skeletal CT scans can provide a valuable resource, granted they are able to present the same information as accurately as if they were dry bones. Another advantage of CT scanning technology is that they have the potential to give more accurate representation of the true diversity of modern individuals than is embodied in dry bone skeletal collections.

One of the limitations of CT scans in research and forensic investigation is the expense of the process, resulting in limited accessibility of CT scanning technology. Not all Medical Examiners offices or research facilities have access to CT scanners. Another possible limitation that can occur in CT scans is the reactivity of the technology to metals. For example, if the subject has metal dental restorations, surgical implants, or metal from ballistic fragments within their body, they will appear distorted on the scan (Carew and Errickson 2019; Katsumura *et al.* 2016). As observed in Skull 8 in the current study which exhibits this distortion on the maxillary and mandibular molars (Figure 2.2).

Figure 2.2. Maxillary (top) and mandibular (bottom) dentition of Skull 8. Note the distortion caused by metal dental restorations in the CT scans.

The original purpose of CT scanning technology was for medical imaging (Bhattacharyya 2016). Since the invention of this technology by Sir Godfrey Hounsfield in 1972, the applications of CT scans have expanded in medicine as well as proving useful to many other fields, such as forensics, biological anthropology, facial approximation, and paleoanthropology.

Medical research using CT images of bones can have relevance to forensic research due to the validation they can provide. A study derived using fleshed cadaver heads to study the feasibility of using CT scans for traumatic craniofacial surgeries, the authors found that he measurements were found to not have a statistically significant difference and therefore, CT scan-derived measurements are claimed to be accurate enough for planning craniofacial surgery after the event of trauma (Cavalcanti *et al.* 1999). The study by Cavalcanti *et al.* (1999) found that most measurements had standard deviations under 1.2 millimeters, meaning that if applied to the forensic anthropological standard acceptable variation of two millimeters (Tallman; pers. comm.), CT measurements should be adequate for research and investigation. Further studies of CT scan measurements for use in craniofacial surgeries have corroborated this indication (Waitzman *et al.* 1992a; Waitzman *et al.* 1992b). Adding another degree of removal from the original skull dimensions, 3D printed skulls have also been found to be accurate enough to use as a model to build custom prosthetics for craniofacial surgeries (Zheng *et al.* 2019).

In addition to the applications of CT scans in medicine, they have also been found to be useful in biological anthropology to study past humans and hominids. In many cases, CT scans are needed to view or study ancient materials without damaging them. One example is the analysis of the bones of mummified remains using CT scanning technology, which has been occurring since the 1970s (Villa and Lynnerup 2020). It would be incredibly destructive and impractical to remove the desiccated soft tissue since the skin and clothing themselves hold invaluable, irreplaceable information. CT scans provide a way to minimize damage while still accessing skeletal data, although the system settings used in clinical settings for the penetration and living tissues must be altered for use on mummified remains (Villa and Lynnerup 2020).

CT scans have also been used to examine trepanned skulls from pre-Colombian Peru (Chege *et al.* 1996). The authors found that CT scans worked well at visualizing healing and new bone formation, and in one case the CT scan actually showed bone remodeling better than gross examination. CT scans could not, however, distinguish postmortem versus antemortem trepanation, and therefore the authors concluded that gross examination is the most desirable method of examination, although CT scans can be nearly as effective on ancient skeletal materials. Micro-CT scanning is also useful in studying patterns of attritional stress in past (and present) peoples (Marchewka *et al.* 2014). Micro-CT scanning can be used to visualize linear, pit, and groove enamel hypoplasia and estimate the length of the stress period that caused the hypoplasia and the periods between stress episodes.

Fossil hominids have also been analyzed using CT scans. This allows delicate fossils to be studied in detail without the need for much handling, which can be detrimental. Elliott *et al.* (2014) studied the accuracy of equations for estimating the body mass of fossil hominins using CT data from modern humans. They have also been used to help estimate endocranial volume of fossil hominids such as *Australopithecus africanus* (Neubauer *et al*. 2012). As with most fossil samples, the subjects used in this study were largely incomplete and the sample size was very small (only five fragmented adult individuals). To fill in the missing data, mirror imaging and semilandmark-based geometric morphometrics were used.

As well as the study of living humans and early humans, CT scans are often used to visualize the internal structures of deceased modern humans for forensic and research purposes. CT scans are particularly useful because they allow access to inner soft and hard tissue structures without having to cut open or macerate the individual. This type of analysis is typically called “virtopsy” or virtual autopsy (Thali *et al.* 2003; Aghayev *et al.* 2008; Lo Re *et al.* 2018). Virtopsy can be very practical for forensic anthropological analysis in cases where traditional autopsy is against the family or individual’s religious beliefs, there is not time or desire to macerate the individual to access the bones, or the information needs to be analyzed in a location where it is not practical to possess or transport remains. Although some cardiac, pulmonary, and microscopic causes of death are difficult to visualize in postmortem CT scans (Aalders *et al.* 2017; Cressey 2010; Joshi *et al*. 2018), they have been found to be an effective tool for detecting and clearly visualizing bone injuries (Thali *et al.* 2003; Dedouit *et al*. 2014; Joshi *et al*. 2018) and pathologies (Dedouit *et al*. 2014). This technology can be particularly useful when the remains are charred, heavily decomposed, mutilated, fragile, or encased in a matrix such as concrete.

A case example of the utility of virtopsy involves forensic anthropological analysis of a body that was found severely burned after a house fire (Dedouit *et al.* 2007). The individual was missing several elements, including the head and distal limbs. After autopsy but prior to maceration, a CT scan was taken of the body. An attempt was made to assess biological profile elements such as age, sex, stature, and ancestry using forensic anthropological methods, analysis of which were then compared to conventional dry bone analysis after maceration. Sex estimation based off of pelvic morphology yielded a sex estimation of male, union of the iliac crests, pubic symphysis analysis, and degenerative osteoarthritis yielded an estimation that the individual was an older adult, and stature estimation using spinal measurements was estimated to be 163 centimeters. Ancestry estimation was attempted using sacral measurements, but results were inconclusive. The individual was identified as the homeowner, and sex and age estimates were found to be correct; however, the stature was underestimated. Flaws in analyses relying on metric variables were predictable because measurements should not be taken on burned bone because of dimensional changes (Thompson 2005). Ultimately, the CT scan actually granted more information than the conventional forensic anthropological analysis, since the fragile charred bone got damaged during preparation. This case illustrates some of the advantages of virtopsy in forensic casework.

Postmortem CT scans have many potential applications in forensic anthropological analysis, such as evaluation of biological profile elements such as sex, age, ancestry, and stature, matching weapon shape and type to 3D rendered bone injuries, bullet trajectory determination, other trauma analysis, analysis of taphonomy, measurement, 3D printing replicas for research or courtroom use, and presentation of remains in a courtroom setting (Carew and Errickson 2019; Christensen *et al.* 2018). Because of this plethora of uses, many forensic studies focus on the application of CT scans in the analysis of skeletal materials.

On intact bodies, postmortem CT scans can provide skeletal information without the need to macerate the body, which saves time. There are also many advantages of taking CT scans of dry bone-only samples, such as convenient transfer and storage of information, digital reconstruction of fragmented bone, postmortem and antemortem comparison, the ability to preserve and work with evidence without damage, and presentation of analyses in court without needing to present the physical remains. For these purposes, Christensen *et al.* (2018) recommend that industrial rather than medical CT scanners be used due to their smaller size, affordability, and clearer imaging due to higher spatial and contrast resolution. However, to use information taken from virtopsy or skeletal CT scans in court, error must be known according to *Daubert* standards.

A few studies to date have compared error rates of measurements taken on bone to those taken on CT scans. Zech *et al.* (2012) used metric analysis of the sacrum to develop a discriminant function equation to estimate sex from sacral measurements taken from CT scans, and then compared the measurements to dry bone measurements taken with calipers. While the equations had only moderate accuracy in predicting sex, it was found that the measurements taken on the CT scans were accurate and comparable to dry bone measurements using independent t-tests for each measurement. Stull *et al.* (2014) produced similar results, comparing measurements taken from a full-body CT scan prior to autopsy to measurements taken of the individual elements after maceration. The bones themselves were then CT scanned as well in order to compare the performance of dry bone measurements, fleshed CT scan measurements, and dry bone CT scan measurements using Bland-Altman plots and percent differences to assess disparities. Results showed that there was only 1.4-2.9% error between data sources, and the measurement methods were generally within two millimeters of each other. Overall the study found that there were minimal differences between sources of measurement data and high intra-observer accuracy, making CT scans a good source for gathering metric information.

A similar study was undertaken by Colman *et al.* (2019) in which cadavers were subjected to CT scans and then processed to obtain dry isolated os coxae in order to assess the accuracy of measurements taken from intact body CT scans versus dry bone CT scans. Results showed that the dry bone CT scan dimensions were slightly larger than the intact CT scan dimensions, which may be due to difficulty in visualizing osteometric landmarks designed for dry bones in intact CT scans. This issue likely would be present in some degree for many of the bones in the human body, and before dry bone CT scans can be used in research these error rates should be studied more and reliably determined. Despite variable or unknown error rates, however, because of the apparent accuracy of skeletal measurements taken in medical and postmortem research, dry bone CT scans are extensively used in forensic anthropological research.

Since building a biological profile is a key part of forensic examination, the use of CT scans in estimation of age, ancestry, sex, and stature has been researched extensively, on both fleshed and dry bone samples. These non-comparative studies which use only CT scans (without comparing them to dry bone) operate under the assumption that there is no significant difference between traditional skeletal analysis and analysis of CT scans of skeletal material. Examples of biological profile studies using only CT scans as a sample include a study by Herrera and Tallman (2019), which developed canonical discriminant functions for differentiating the ancestral groups from the Dominican Republic and Haiti, and a study by Zhan *et al.* (2019) which developed discriminant function and regression equations for the estimation of sex and stature of Chinese individuals. Both of these studies used only cranial measurements taken from CT scans, and both studies were successful in using their respective measurements to create accurate, useful equations which can be used in forensic casework to aid in identification.

Researchers have also found success correlating CT scan measurements of teeth to age, specifically the pulp-to-tooth ratio of maxillary canines (Rai *et al.* 2016) and measurements of the third molar (Bassed *et al.* 2011). Correlations have also been found of CT scan measurements of orbital muscles and interzygomatic distances to age and sex (Ozgen and Ariyurek 1998), medial clavicle to age, even in young individuals (Bassed *et al.* 2011), and stature based on skeletal and skull measurements (Giurazza *et al.* 2012). Additional studies regarding the use of CT scans in sex estimation have been found valid using measurements of volume-rendered and surface-rendered CT scans of living people (Simmons-Ehrhardt *et al.* 2019; Ramsthaler *et al.* 2010). Metric ancestry estimation has also been validated using cranial CT scan measurements in living individuals entered into a FORDISC-like program developed by the Federal Bureau of Investigation called ReFace (Simmons-Ehrhardt *et al.* 2019).

CT scans can allow for visual and spatial analysis of the exterior as well as interior structures of bone. For example, they can be used to view the frontal sinus. Frontal sinus features noted in a study by Uthman *et al.* (2010) included presence or absence of a frontal sinus, septum, and scalloping, as well as measurements between the two highest points on the frontal sinus and the distance between the highest points and the maximum lateral limit. Uthman *et al.* (2010) found that the features and measurements of the frontal sinus were useful in sex estimation, although the accuracy of this was improved with the addition of skull measurements. Bones other than the cranium can be used for identification as well. Postmortem CT scans allow anatomical features, skeletal pathologies, surgical intervention, sex, and stature to be viewed and assessed (Hishmat *et al.* 2014). These postmortem CT scans can then be compared to antemortem CT scans, x-rays, written records, and other kinds of images, providing positive identification or at the very least narrowing down the pool of possible matches.

Aside from biological profile and identification information, trauma analysis is also an important aspect of forensic analysis. Fractography, or the study of fracture surface morphology, has been studied using CT scans (Christensen and Hatch 2019). Researchers analyzed images of fractured femora to see if diagnostic features such as bone mirror, cantilever curl, bone hackle, wake features, and arrest ridges are visible on the CT scans. These features can be used to estimate how cracks formed and spread as well as impact directionality. The researchers found that although finer details were lost in the CT scan, fracture propagation and impact direction could still be determined and therefore, CT scans of fractured bone have forensic potential for application. Similarly, CT scans have proven useful in the analysis of blunt force trauma, with radiologists able to determine the shape of the weapon, number of blows, and location of fractures based on 2D and 3D CT images of crania (Bakker *et al.* 2013; Combrinck and Vuuren 2017). This information can be used for corroboration of case information, determination of cause and manner of death, murder weapon, demonstrative information for court use, and reconstruction of events.

Villa *et al.* (2017) studied the potential for the application of full-body postmortem CT scans and partial CT scans of injuries in 3D reconstructions of occurrences surrounding injurious events linked to crimes. These variables include bullet paths, trauma, wound depth, and potential weapons. These 3D models can be built using full body postmortem CT scans and reconstructing the probable positioning of the individual during the event. This can also be used to corroborate forensics events involving traumatic injuries caused living people to reconstruct events for corroboration from live CT. This study used the full-body postmortem CT scan of an individual that died from gunshot wounds and a full-body reconstruction from multiple partial body CT scans from a gunshot victim that survived their wounds. The authors were able to demonstrate that CT scans of living and deceased individuals can be used to recreate body positioning in injurious events.

2.5 Conclusion

In conclusion, from contentious beginnings to the high-tech present and future, analysis of ancestry and sex using anthropological methods can be done using a plethora of methods. To estimate sex and ancestry, methods include the rudimentary practice of merely observing morphological traits, morphological analysis using trait scores paired with logistic regression analysis, automated morphological analysis, and automated metric analysis. These methods can apply to almost every element in the human skeleton, although the skull is often the focus of such analyses. These methods are constantly being retested and validated on different populations, adding to the myriad number of specialized discriminant functions designed to give the most accurate results, often for the purpose of aiding in forensic casework.

These forensic anthropological methods, among other methods of building a biological profile to aid in identification, have been tested on and applied to samples of dry bone, CT scans of intact, fleshed cadavers, CT scans of charred remains, CT scans of living humans, and CT scans of dry bone. Comparison studies between dry bone analysis and various types and conditions of CT scans have performed well, and the current study aims to build upon this past work, confirming the reliability and utility of morphological and metric data gathered from CT scans in forensic casework and research.

Chapter III: MATERIALS AND METHODS

3.1 Materials

For this study, eight skulls of donor individuals from the Boston University forensic anthropology skeletal collection were used. The individuals used were BU-41, BU-40, BU-39, BU-38, BU-34, BU-33, BU-31, and BU-30, which were relabeled for the purposes of this study as Skull 1, Skull 2, Skull 3, Skull 4, Skull 5, Skull 6, Skull 7, and Skull 8, respectively (Table 3.1). This renaming was for the purpose of simplicity. Table 3.1 also includes the donor individuals' actual sex, ancestry, and age. Photos of each skull used in this study are included in Figures 3.1-3.8.

Table 3.1. Skull name designations for the purpose of this study and actual sex, ancestry, and age of donor individuals.

Name designation	Donor	Sex	Ancestry	Age at Death
Skull 1	BU-41	Male	White	67
Skull 2	BU-40	Female	White	71
Skull 3	BU-39	Male	White	70
Skull 4	BU-38	Female	White	70
Skull 5	BU-34	Male	White	74
Skull 6	BU-33	Female	White	81
Skull 7	BU-31	Male	White	67
Skull 8	BU-30	Female	White	73

Figure 3.1. Skull 1. Anterior view, left lateral view, and superior view of mandible.

Figure 3.2. Skull 2. Anterior view, left lateral view, and superior view of mandible.

Figure 3.3. Skull 3. Anterior view, left lateral view, and superior view of mandible.

Figure 3.4. Skull 4. Anterior view, left lateral view, and superior view of mandible.

Figure 3.5. Skull 5. Anterior view, left lateral view, and superior view of mandible.

Figure 3.6. Skull 6. Anterior view, left lateral view, and superior view of mandible.

Figure 3.7. Skull 7. Anterior view, left lateral view, and superior view of mandible.

Figure 3.8. Skull 8. Anterior view, left lateral view, and superior view of mandible.

The other materials used in this study were a Philips IQon Spectral CT scanner used to take CT scans of the donor skulls (provided on a set of discs by Boston Medical Center), a digital sliding calipers (BUDC-04), a digital spreading calipers (BUDC-07), a mandibulometer, and RadiAnt 5.5.1 64-bit CT scan viewer (as used in Herrera and Tallman 2019).

3.2 CT Scans

The eight skulls of donor individuals were CT scanned using the Philips IQon Spectral CT scanner at Boston Medical Center. The skulls were each lined up on the CT bed with the mandibles placed posteriorly to their respective crania, and the crania were held up on cork rings with the basicrania facing anteriorly. The crania and mandibles were kept steady with medical tape designed to not interfere with radiographic scanning. Katsumura *et al.* (2016) compared cone beam CT scans with helical CT scans of three skulls, and cone beam CT scans were found to be more accurate, although both CT scan types produced images close in accuracy to dry bone analysis. It is also recommended by researchers to use at least a 64 multi-slice scanner (Bakker *et al.* 2013). For the purposes of this study, helical CT scanning was used, as that was the type of equipment available.

The CT scan yielded the 3D-rendered skull images needed for the purposes of analysis (Figures 3.9-3.16). Most of the resulting CT scans were incomplete in some way, with thinner areas of bone not appearing on the scan and subsequently not appearing in the digital rendering. For example, all mandibular condyles except for those of Skull 1 (Figure 3.9) did not appear. Other thin areas, such as the areas around the nasal aperture and the orbits, did not appear on all of the CT scans except for Skull 1 (Figures 3.10-3.16).

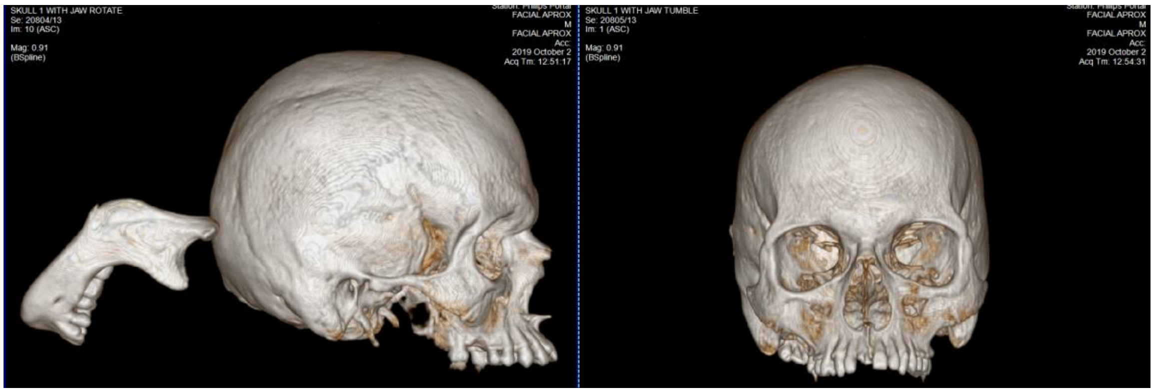

Figure 3.9. CT scan of skull 1. Left lateral and anterior views.

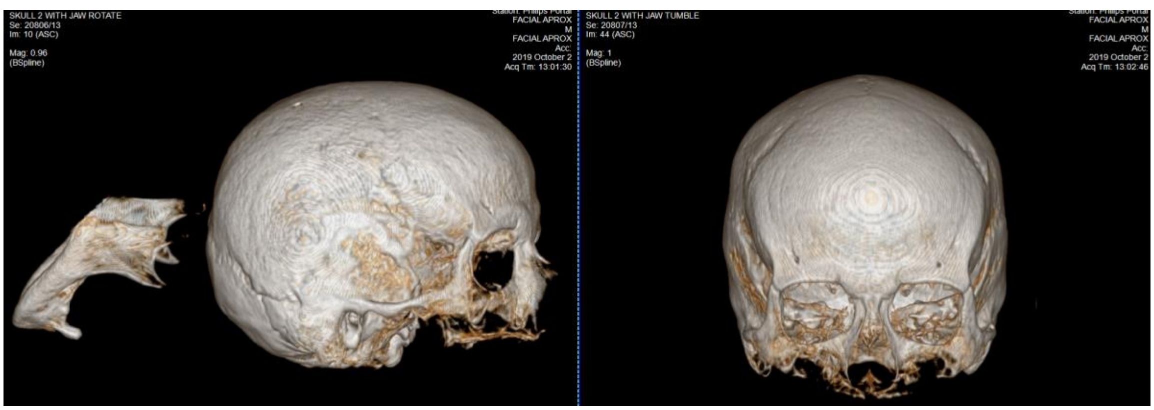

Figure 3.10. CT scan of skull 2. Left lateral and anterior views.

Figure 3.11. CT scan of skull 3. Left lateral and anterior views.

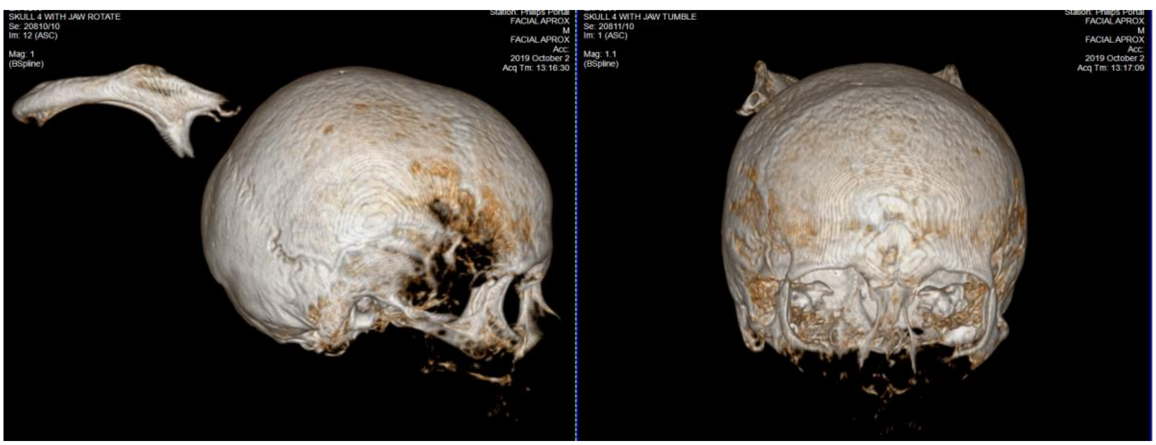

Figure 3.12. CT scan of skull 4. Left lateral and anterior views.

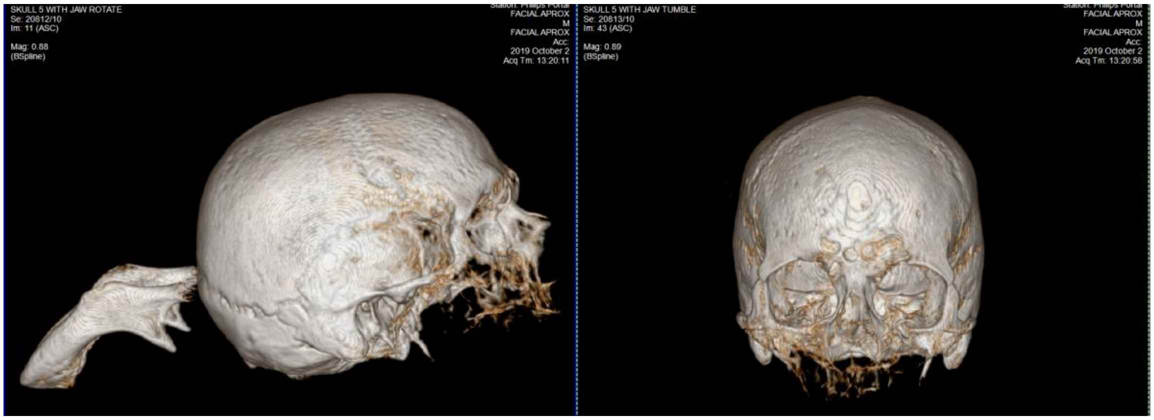

Figure 3.13. CT scan of skull 5. Left lateral and anterior views.

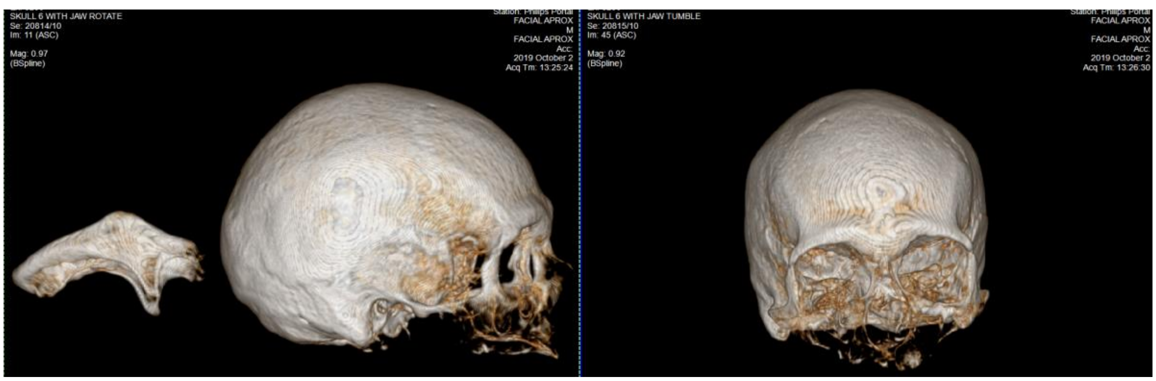

Figure 3.14. CT scan of skull 6. Left lateral and anterior views.

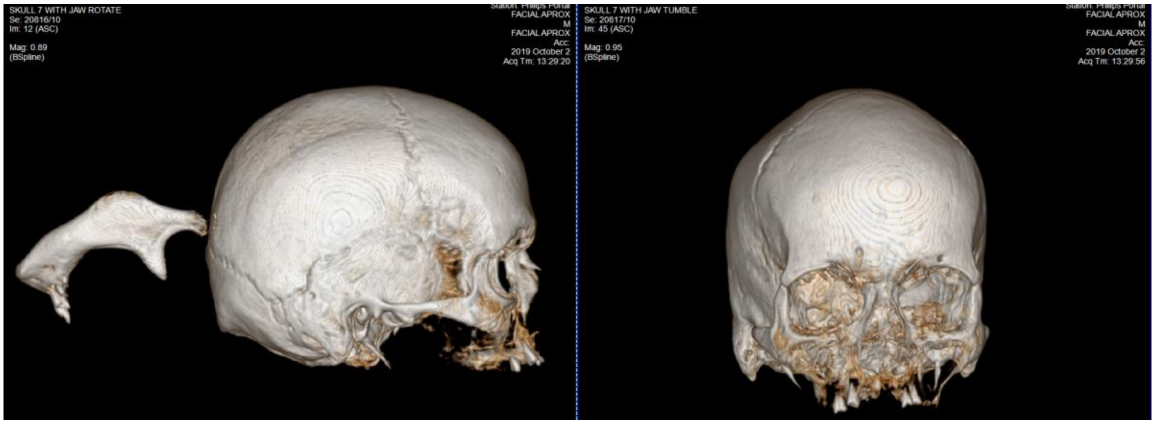

Figure 3.15. CT scan of skull 7. Left lateral and anterior views.

Figure 3.16. CT scan of skull 8. Left lateral and anterior views.

Consequently, measurements dependent on missing areas were not included in the analyses of measurement differences, morphological comparison, or FORDISC 3.1 analyses. These measurements not taken in the CT scan sample were removed from the dry skull measurement data as well for the purpose of one-to-one comparison. In addition, the coronal, sagittal, and occipital sutures on some of the skulls were poorly defined, which made the landmarks asterion, bregma, and lambda more difficult to visualize on the CT scans (Figure 3.17). Therefore, the CT scan resolution may have feasibly affected the ability to accurately take measurements of the biasterionic breadth, frontal chord, occipital chord, and parietal chord, which rely on those landmarks. However, since the sutures are still somewhat visible, these measurements were not omitted.

Figure 3.17. Skulls 6 (left) and 8 (right), superior view. Note the poorly defined coronal, sagittal, and occipital sutures.

3.3 Morphological Methods

The focus of morphological comparison in this study was the use of popular cranial sex and ancestry estimation techniques and whether they can be applied effectively when used with CT scans of skulls rather than traditional dry skull analysis. Morphological traits for sex were scored following Walker (2008) and morphological traits for ancestry were scored following Hefner and Ousley (2014).

For morphological sex estimation, the nuchal crest, mastoid process, supra-orbital margin, glabella, and mental eminence of each skull and CT scan were scored based on robusticity using the five-value ordinal scoring scale provided in Walker (2008) (Figure 3.18). Analysis of the dry skulls was conducted in-person at the Boston University Medical Campus using traditional morphological observation practice. The analysis of the traits on the CT scans was conducted using RadiAnt 5.5.1 64-bit CT viewer, which allowed for the 3D volume rendered CT scan images to be moved into positions conducive to viewing the morphology of the nuchal crest, mastoid process, supra-orbital margin, glabella, and mental eminence on a 2D screen. Ordinal scores for each trait were then compared for percent differences. Easiest to score on the CT scans were the traits viewable on the lateral plane, such as the nuchal crest, mastoid process, and glabella. Scoring for the mental eminence was also straightforward; however, scoring the supra-orbital margin was difficult on the CT scans since when scoring the actual skull, this trait is often scored not only visually but by manually feeling the thickness. This was plainly not possible on the CT scans, and may have resulted in some error in scoring that trait.

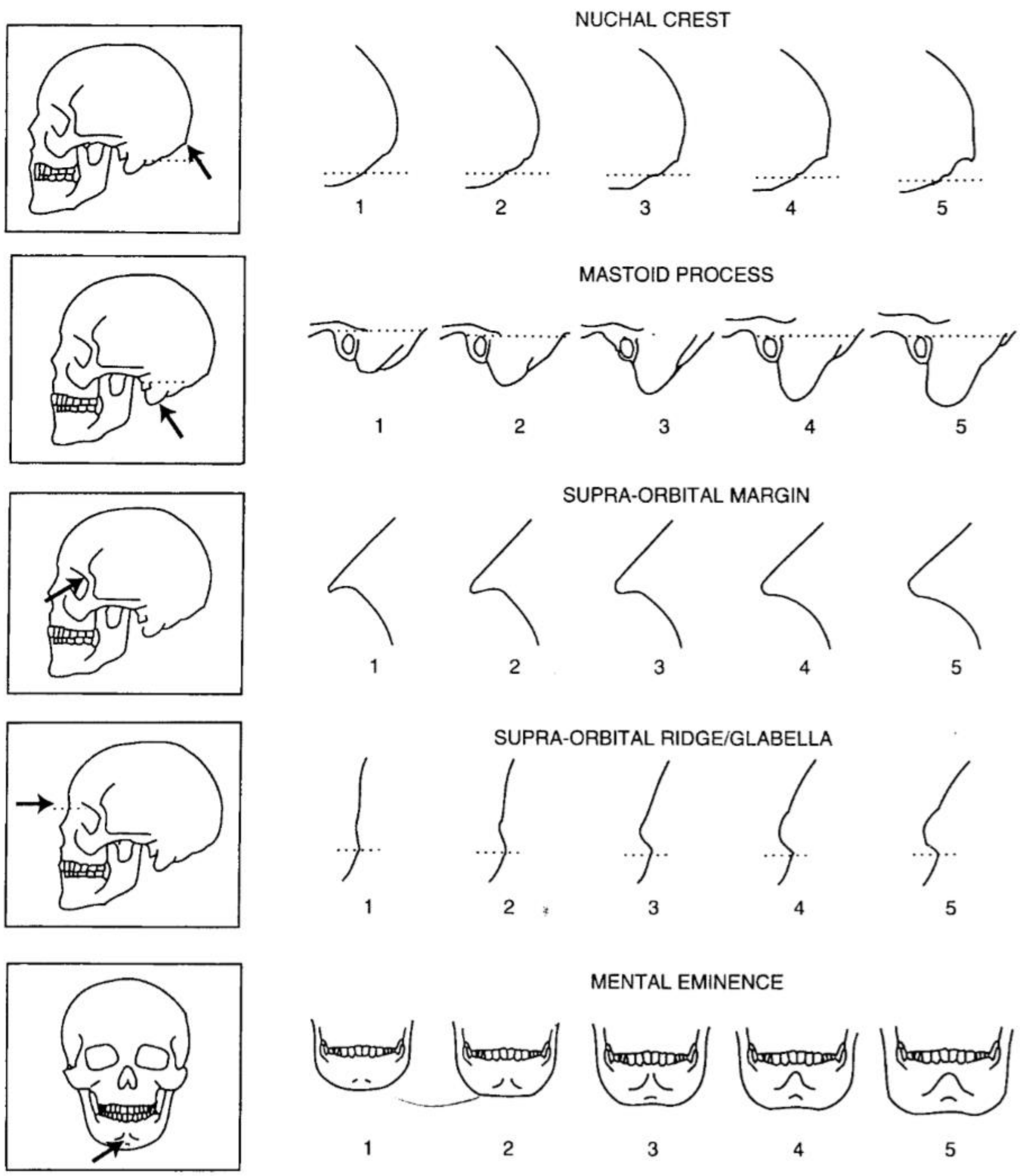

Figure 3.18. Cranial morphological character states from Buikstra and Ubelaker (1994:20).

The ordinal scores for each skull and CT scan were then entered into Walker's (2008) logistic discriminant analysis equations, which output a Y-value. If this Y-value is greater than zero (positive), the skull is more likely to be female and if the Y-value is less than zero (negative), the skull is more likely to be male. The resultant sex estimations for each dry skull-to-CT scan pairing were then compared for discordant outcomes.

For morphological estimation of ancestry, Hefner and Ousley's (2014) OSSA method was used. For this method, six cranial morphological traits are scored following the guidelines in Hefner (2009). Each trait has unique criteria for scoring the character states, unlike the gracile-to-robust range of scoring in Walker (2008) and Buikstra and Ubelaker (1994). Traits scored for ancestry include the anterior nasal spine (1-slight, 2-intermediate, 3-marked) (Figure 3.19), inferior nasal aperture (1-pronounced slope, 2-moderate slope, 3-straight, 4-partial sill, 5-sill) (Figure 3.20), interorbital breadth (1-narrow, 2-intermediate, 3-wide) (Figure 3.21), nasal aperture width (1-narrow, 2-medium, 3-broad) (Figure 3.22), nasal bone structure (0-low/round, 1-oval, 2-marked plateau, 3-narrow plateau, 4-triangular) (Figure 3.23), and post-bregmatic depression (0-absent, 1-present) (Figure 3.24).

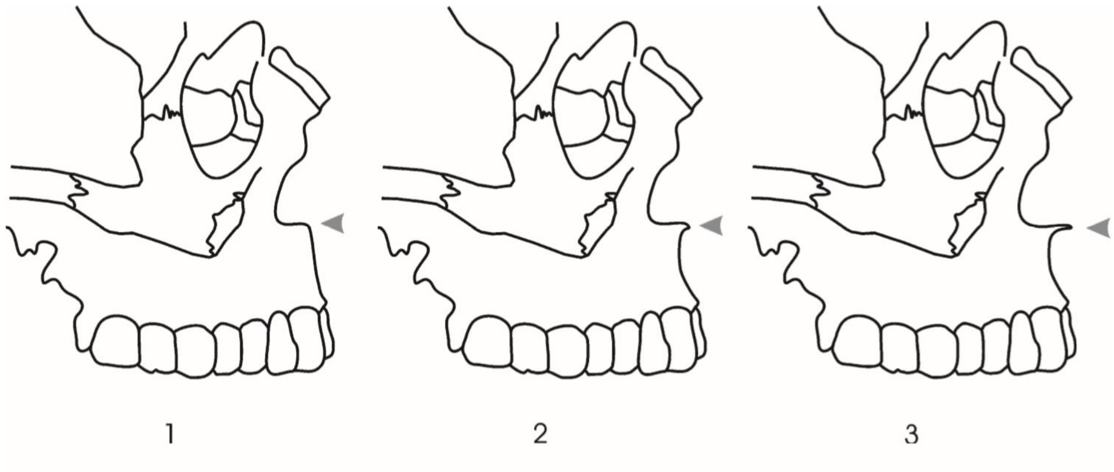

Figure 3.19. Anterior nasal spine character states from Hefner (2009:987).

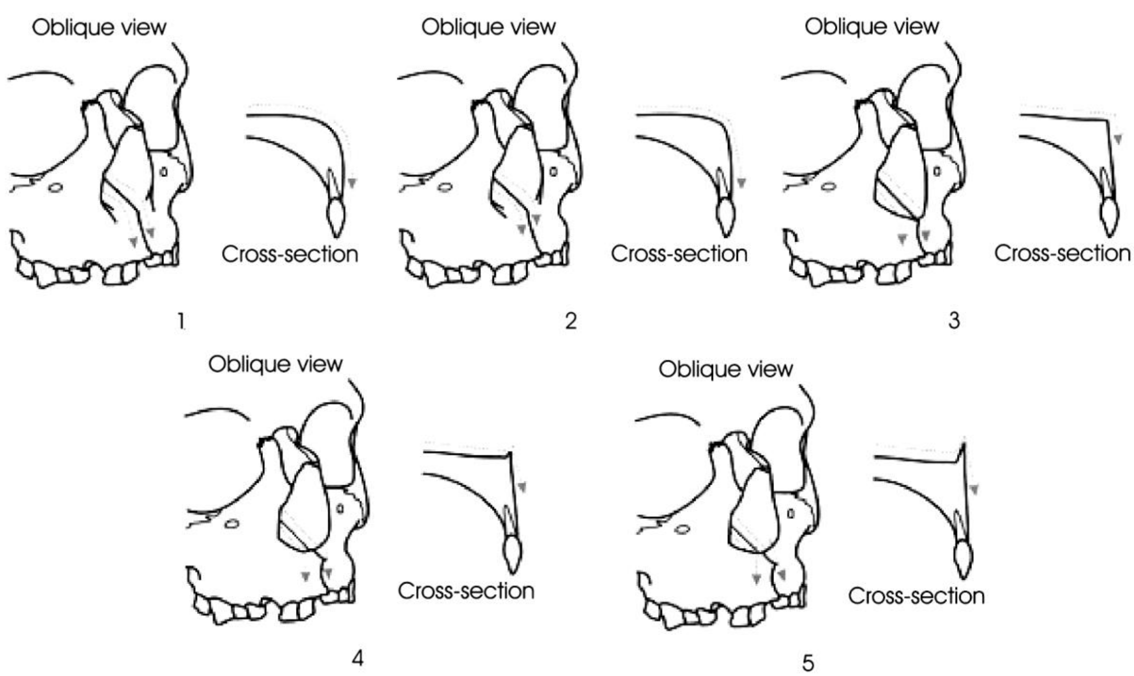

Figure 3.20. Inferior nasal aperture character states from Hefner (2009:988).

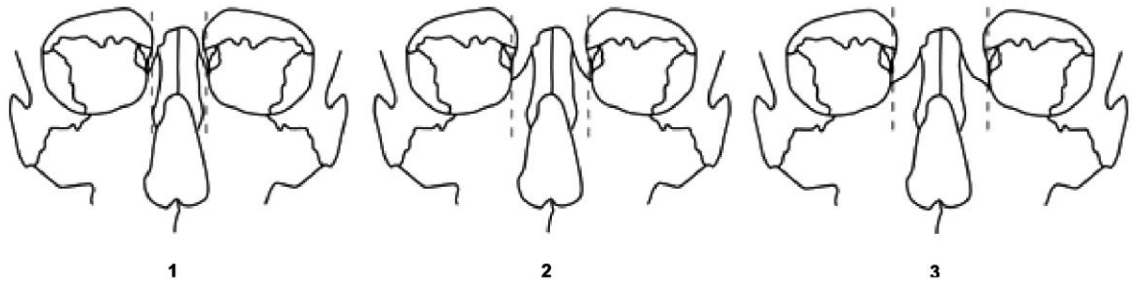

Figure 3.21. Interorbital breadth character states from Hefner (2009:988).

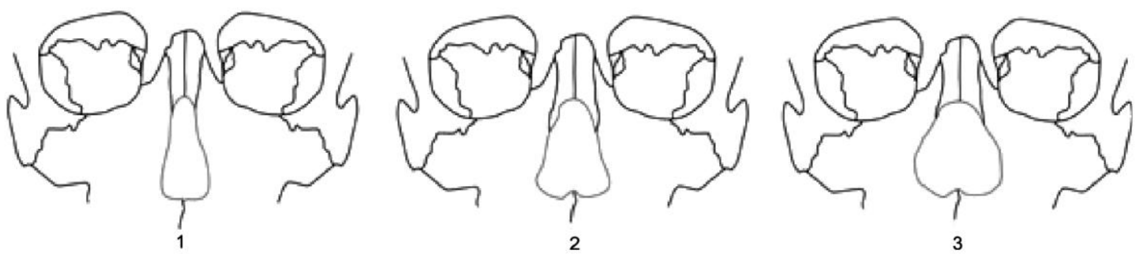

Figure 3.22. Nasal aperture width character states from Hefner (2009:989).

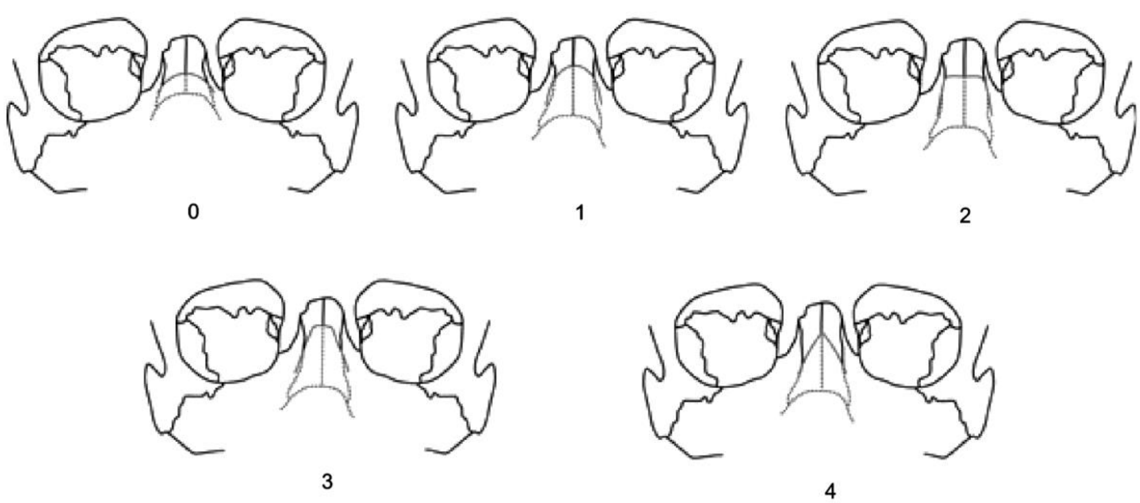

Figure 3.23. Nasal bone structure from Hefner (2009:989).

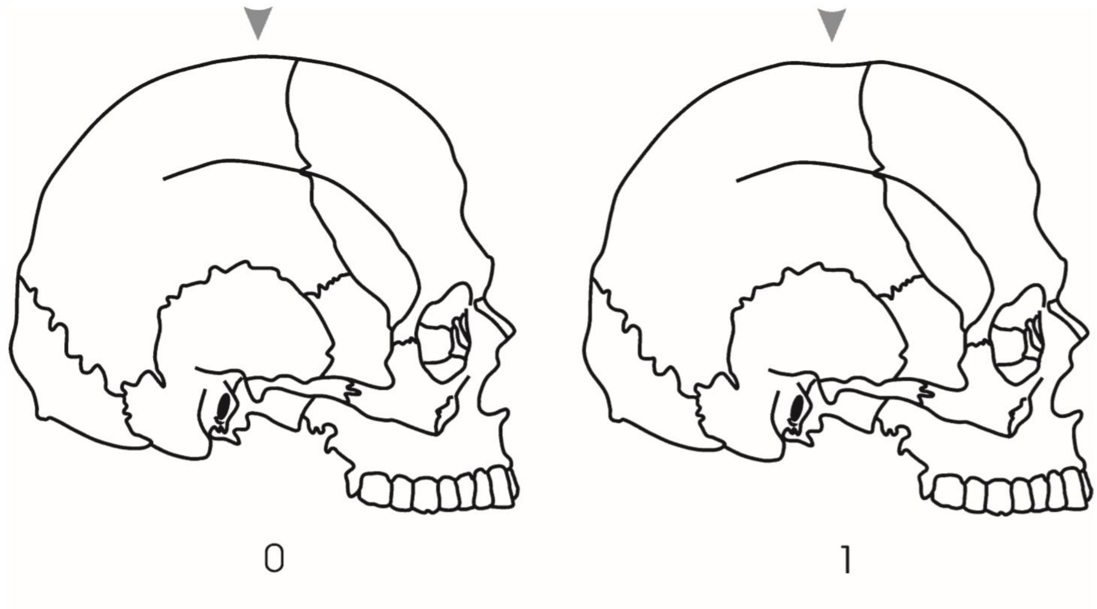

Figure 3.24. Post-bregmatic depression character states from Hefner (2009:990).

These character state scores each correspond to an OSSA score of one or zero, which are included in the OSSA chart (Figure 3.25). The OSSA scores for each trait were then summed, and the overall score corresponds to the most likely ancestral group and strength of correlation (given the individual is of African- or European- derived ancestry).

Anterior Nasal Spine (ANS)

State	OSSA		
1	0	Slight	
2	1	Intermediate	
3	1	Marked	ANS State =
			OSSA SCORE =

Nasal Aperture Width (NAW)

State	OSSA		
1	1	Narrow	
2	1	Medium	
3	0	Broad	NAW State =
			OSSA SCORE =

Inferior Nasal Aperture (INA)

State	OSSA		
1	0	Pronounced Slope	
2	0	Moderate Slope	
3	0	Straight	
4	1	Partial Sill	
5	1	Sill	INA State =
			OSSA SCORE =

Nasal Bone Structure (NBS)

State	OSSA		
0	0	Low/Round	
1	0	Oval	
2	1	Marked Plateau	
3	1	Narrow Plateau	
4	1	Triangular	NBS State =
			OSSA SCORE =

Interorbital Breadth (IOB)

State	OSSA		
1	1	Narrow	
2	1	Intermediate	
3	0	Wide	IOB State =
			OSSA SCORE =

Post-Bregmatic Depression (PBD)

State	OSSA		
0	1	Absent	
1	0	Present	
			PBD State =
			OSSA SCORE =

SUMMED OSSA SCORE =

Race Assessment: ______________ Percent Correct (for sample): ____________%

Figure 3.25. OSSA scoring table from Hefner and Ousley (2014:4).

Results from the individual ancestral trait scores were then analyzed for differences, expressed as a percentage when applicable, and the overall ancestry estimations for each dry skull-to-CT scan pairing were compared for discordant outcomes.

3.4 Metric Methods

Standard craniometric measurements were taken on each skull following the instructions for standard cranial measurements in Langley *et al.* (2016). These measurements rely on knowledge and accessibility of landmarks on the skull (Table 3.2) and the ability to measure the linear distance between them with physical and digital tools. This was achieved on the dry skulls using digital sliding calipers BU-04, digital spreading calipers BU-07, and mandibulometer, with measurements rounded to the nearest millimeter. Due to Skulls 4, 5, and 6 being fully edentulous (Figures 3.4, 3.5, 3.6, 3.12, 3.13, and 3.14) and Skulls 2 and 7 missing teeth in areas affecting measurements (Figures 3.2, 3.7, 3.10, and 3.15), the cranial and mandibular measurements reliant on landmarks affected by tooth loss and alveolar resorption (basion-prostheon length, maxillo-alveolar breadth, maxilla-alveolar length, nasion-prostheon height, chin height, height of the mandibular body, breadth of the mandibular body, and maximum ramus breadth) were omitted from the data.

Table 3.2. Cranial landmarks. Adapted from Langley *et al.* (2016).	
Landmark	**Description**
Alveolon (alv)	The point where the mid-sagittal plane of the palate is intersected by a line connecting the posterior borders of the alveolar crests.
Asterion (ast)	The point where the temporal, parietal, and occipital bones meet.
Basion (ba)	The point at which the anterior border of the foramen magnum is intersected by the mid-sagittal plane opposite nasion.
Bregma (b)	The posterior border of the frontal bone in the mid-sagittal plane.
Condylion (cdl)	The most lateral points of the mandibular condyles.
Dacryon (d)	Dacryon is located on the frontal bone. When the lacrimomaxillary suture is easily found, dacryon is the point on the frontal bone where the frontal, lacrimal and maxillary sutures meet.
Ectoconchion (ec)	The intersection of the most anterior edge of the lateral orbital border and a line parallel to the superior orbital border that bisects the orbit into two equal halves.
Ectomolare (ecm)	The most lateral point on the buccal surface of the alveolar margin.
Euryon (eu)	The most laterally positioned point on the side of the braincase.
Frontomalare temporale (fmt)	The most laterally positioned point on the fronto-malar suture.
Frontotemporale (ft)	A point located generally forward and inward on the superior temporal line directly above the zygomatic process of the frontal bone.
Glabella (g)	The most anteriorly projecting point in the mid-sagittal plane at the lower margin of the frontal bone, which lies above the nasal root and between the superciliary arches.
Gnathion (gn)	The lowest point on the inferior margin of the mandibular body in the mid-sagittal plane.
Gonion (go)	The point on the mandible where the inferior margin of the mandibular corpus and the posterior margin of the ramus meet, i.e. the point on the mandibular angle which is directed most inferiorly, posteriorly, and laterally.
Infradentale (id)	The point between the lower incisor teeth where the anterior margins of the alveolar processes are intersected by the mid-sagittal plane.
Lambda (l)	The apex of the occipital bone at its junction with the parietals, in the midline.
Mastoidale (ms)	The most inferior point on the tip of the mastoid process.
Nasion (n)	The point of intersection of the naso-frontal suture and the mid-sagittal plane.
Opisthocranion (op)	The most distant point posteriorly from glabella on the occipital bone, located in the mid-sagittal plane.
Opisthion (o)	The point on the inner border of the posterior margin of the foramen magnum in the mid-sagittal plane.
Prostheon (pr)	The most anterior point on the alveolar border of the maxilla between the central incisors in the mid-sagittal plane.
Porion (po)	The most superior point along the upper margin of the external acoustic meatus.
Radiculare (ra)	The point on the lateral aspect of the root of the zygomatic process at the deepest incurvature.
Zygion (zy)	The most laterally positioned point on the zygomatic arches.
Zygomaxillare anterior (zma)	The intersection of the zygomaxillary suture and the limit of the attachment of the masseter muscle, on the facial surface.
Zygoorbitale (zo)	The intersection of the orbital margin and the zygomaxillary suture.

In the CT scans, measurements were taken using the RadiAnt 5.5.1 64-bit CT viewer, also to the nearest millimeter. The measurement tool within the program defaults to pixels as a unit of measurement, with a 10 cm scale on the side. The digital measurement tool was calibrated to measure in millimeters using the 10-centimeter bar as a reference. Measurements of basion-bregma height and cranial base length were not taken in the CT sample due to the inability to view basion at the same time as bregma or nasion in the digital rendering. In all the CT scans except for that of Skull 1 (Figure 3.9), the mandibular condyles did not show up, so all measurements relying on the mandibular condyles were also omitted.

All standard FORDISC 3.1 measurements removed from analysis for any reason include the basion-bregma height (BBH), basion-nasion length (BNL), basion-prostheon length (BPL), palate breadth (MAB), palate length (MAL), upper facial height (UFHT), zygomaxillary breadth (ZMB), nasal breadth (NLB), midorbital width (MOW), chin height (GNI), height at mental foramen (HMF), breadth at mental foramen (TMF), bicondylar breadth (CDL), and maximum ramus height (XRH).

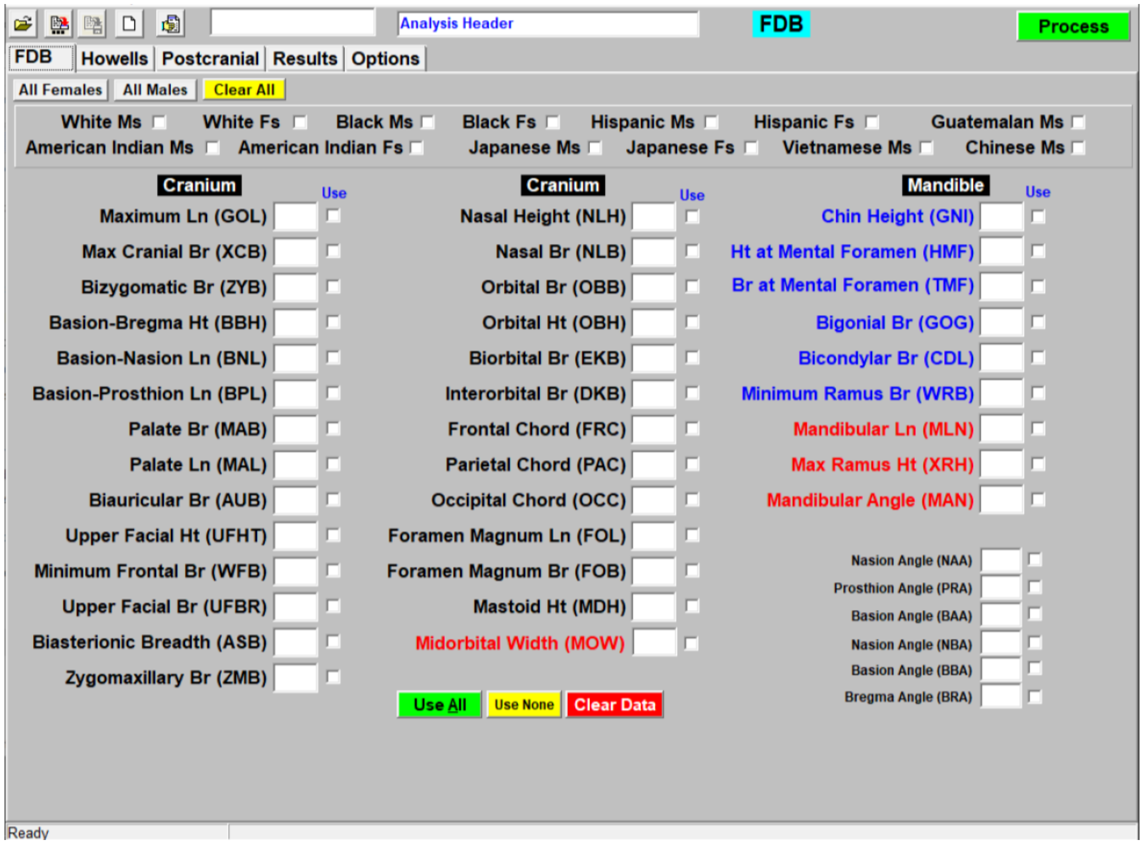

Figure 3.26. FORDISC 3.1 data entry page.

After the omission of problematic measurements, the remaining measurements were entered into the FORDISC 3.1 data entry page (Figure 3.26). Standard FORDISC 3.1 measurements included in analysis were biasterionic breadth (ASB), biauricular breadth (AUB), interorbital breadth (DKB), biorbital breadth (EKB), foramen magnum breadth (FOB), foramen magnum length (FOL), frontal chord (FRC), bigonial breadth (GOG), maximum cranial length (GOL), mandibular angle (MAN), mastoid height (MDH), mandibular length (MLN), nasal height (NLH), orbital breadth (OBB), orbital height (OBH), occipital chord (OCC), parietal chord (PAC), upper facial breadth

(UFBR), minimum frontal breadth (WFB), minimum ramus breadth (WRB), maximum cranial breadth (XCB), and bizygomatic breadth (ZYB). Detailed descriptions of all standard FORDISC 3.1 measurements are included in Table 3.3.

Table 3.3. Measurements used in FORDISC analysis. Adapted from Langley *et al.* (2016).

Measurement	Description
ASB	Biasterionic breadth; ast-ast; straight-line distance from left to right asterion (ast).
AUB	Biauricular breadth; ra-ra; the least exterior breadth across the roots of the zygomatic processes.
BBH	Basion-bregma height; ba-b; the distance from basion (ba) to bregma (b).
BNL	Basion-nasion length (cranial base length); ba-n; the distance from nasion (n) to basion (ba).
BPL	Basion-prostheon length; ba-pr; the distance from basion (ba) to prosthion (pr).
CDL	Bicondylar breadth; cdl-cdl; the distance between the most lateral points on the mandibular condyles (cdl).
DKB	Interorbital breadth; d-d; the distance between right and left dacryon.
EKB	Biorbital breadth; ec-ec; the distance from left to right ectoconchion (ec).
FOB	Foramen magnum breadth; the distance between the lateral margins of the foramen magnum at the point of greatest lateral curvature.
FOL	Foramen magnum length; the mid-sagittal distance from the most anterior point on the foramen magnum margin to opisthion (o).
FRC	Frontal chord; n-b; the distance from nasion (n) to bregma (b) taken in the mid-sagittal plane.
GNI	Chin height; id-gn; the distance from infradentale (id) to gnathion (gn).
GOG	Bigonial breadth; go-go; the distance between the right and left gonion (go).
GOL	Maximum cranial length; g-op; the straight-line distance from glabella (g) to opisthocranion (op) in the midsagittal plane.
HMF	Height at mental foramen (height of the mandibular body); the distance from the alveolar process to the inferior border of the mandible at the level of the mental foramen.
MAB	Palate breadth (maxillo-alveolar breadth) ; ecm-ecm; the maximum breadth across the alveolar borders of the maxilla measured on the lateral surfaces at the location of the second maxillary molars.
MAL	Palate length (maxilla-alveolar length); pr-alv; the distance from prosthion (pr) to alveolon (alv).
MAN	Mandibular angle; the angle formed by inferior border of the corpus and the posterior border of the ramus.
MDH	Mastoid height; the direct distance between porion and mastoidale.
MLN	Mandibular length; the distance from the anterior margin of the chin to the midpoint of a straight line extending from the posterior border of the right and left mandibular angles.
NLB	Nasal breadth; the maximum breadth of the nasal aperture.
NLH	Nasal height; the average height from nasion (n) to the lowest point on the border of the nasal aperture on either side.
OBB	Orbital breadth; d-ec; the distance from dacryon (d) to ectoconchion (ec).
OBH	Orbital height; the distance between the superior and inferior orbital margins perpendicular to orbital breadth and bisecting the orbit into equal medial and lateral halves.
OCC	Occipital chord; l-o; the distance from lambda (l) to opisthion (o) taken in the mid-sagittal plane.
PAC	Parietal chord; b-l; the distance from bregma (b) to lambda (l) taken in the mid-sagittal plane.
TMF	Breadth at mental foramen (breadth of mandibular body); the maximum breadth measured at the level of the mental foramen perpendicular to the long axis of the mandibular body.
UFBR	Upper facial breadth; fmt-fmt; the distance between the right and left frontomalare temporale.
UFHT (NPH)	Upper facial height (nasion-prostheon height); n-pr; the distance from nasion (n) to prosthion (pr).
WFB	Minimum frontal breadth; ft-ft; the distance between the right and left frontotemporale.
WRB	Minimum ramus breadth; the minimum breadth of the mandibular ramus measured perpendicular to the height of the ramus.
XCB	Maximum cranial breadth; eu-eu; the maximum width of the skull perpendicular to the mid-sagittal plane wherever it is located with the exception of the inferior temporal line and the immediate area surround the latter
XRH	Maximum ramus height; the distance from gonion (go) to the highest point on the mandibular condyle.
ZMB	Zygomaxillary breadth (bimaxillary breadth); zma-zma; the breadth across the maxillae, from the left to right zygomaxillare anterior (zma).
ZYB	Bizygomatic breadth; zy-zy; the maximum breadth across the zygomatic arches, wherever found, perpendicular to the mid-sagittal plane.

The measurements from each skull and CT scan were entered into FORDISC 3.1 and run for all male and female populations using the Forensic Database (FDB) dataset. The data then provided by FORDISC 3.1 included statistical distance and probabilities indicating closeness to each group. For traditional metric sex and ancestry estimation, Johnson *et al.* (1990) recommend estimating ancestry before sex, the opposite of what was done in this study due to the nature of FORDISC 3.1 analysis. Typically, the closest several groups will be one sex, and the other sex can then be eliminated. For each skull and CT scan, the closest sex estimation was noted. Then, the lesser-likely sex was eliminated from the FORDISC 3.1 data pool and the measurements were processed again, this time to estimate ancestry. This process was repeated for each set of skull measurements and each set of CT measurements. The FORDISC 3.1 estimations were then compared for each skull-to-CT pairing and any inconsistencies in sex or ancestry were noted.

3.5 Statistical Analysis

The eight skull measurements were compared to the eight CT scan measurements for biasterionic breadth (ASB), biauricular breadth (AUB), interorbital breadth (DKB), biorbital breadth (EKB), foramen magnum breadth (FOB), foramen magnum length (FOL), frontal chord (FRC), bigonial breadth (GOG), maximum cranial length (GOL), mandibular angle (MAN), mastoid height (MDH), mandibular length (MLN), nasal height (NLH), orbital breadth (OBB), orbital height (OBH), occipital chord (OCC), parietal chord (PAC), upper facial breadth (UFBR), minimum frontal breadth (WFB), minimum ramus breadth (WRB), maximum cranial breadth (XCB), and bizygomatic breadth (ZYB) for minimum deviation, maximum deviation, and average deviation, and then analyzed for significant variance using a one-way ANOVA.

A one-way ANOVA produces an F-ratio, which is the ratio of the variance calculated among the means to the variance within the samples. In other words, the F-ratio is the calculation of how much between-group variation is present compared to how much within-group variation is present. Theoretically, the closer the F-ratio is to one, the less difference between the groups in question. The one-way ANOVA also calculates a p-value, which is the value that indicates if the results of the analysis are significant or not. For this study, the alpha for the p-value was decided to be 0.05. If the p-value from the ANOVA is less than 0.05, the groups have significant variance, and if the p-value is greater than 0.05, the variance is insignificant. This one-way ANOVA calculation was undertaken for each measurement.

Chapter IV: RESULTS

4.1 Morphological Sex Estimation Results

Scoring results of the cranial morphological sex traits following Walker (2008) and Buikstra and Ubelaker (1994) for each of the dry skulls and CT scans are included in Figure 4.1.

Dry Skull 1	Left	Center	Right
Nuchal crest (1-5)		3	
Mastoid process (1-5)	4		4
Supraorbital margin (1-5)	3		3
Glabella (1-5)		4	
Mental eminence (1-5)		3	

CT Scan 1	Left	Center	Right
Nuchal crest (1-5)		3	
Mastoid process (1-5)	4		5
Supraorbital margin (1-5)	4		4
Glabella (1-5)		4	
Mental eminence (1-5)		4	

Dry Skull 2	Left	Center	Right
Nuchal crest (1-5)		1	
Mastoid process (1-5)	2		2
Supraorbital margin (1-5)	1		1
Glabella (1-5)		1	
Mental eminence (1-5)		2	

CT Scan 2	Left	Center	Right
Nuchal crest (1-5)		1	
Mastoid process (1-5)	3		2
Supraorbital margin (1-5)	1		1
Glabella (1-5)		2	
Mental eminence (1-5)		2	

Dry Skull 3	Left	Center	Right
Nuchal crest (1-5)		4	
Mastoid process (1-5)	3		4
Supraorbital margin (1-5)	3		3
Glabella (1-5)		4	
Mental eminence (1-5)		5	

CT Scan 3	Left	Center	Right
Nuchal crest (1-5)		4	
Mastoid process (1-5)	3		3
Supraorbital margin (1-5)	3		3
Glabella (1-5)		4	
Mental eminence (1-5)		5	

Dry Skull 4	Left	Center	Right
Nuchal crest (1-5)		1	
Mastoid process (1-5)	1		1
Supraorbital margin (1-5)	1		1
Glabella (1-5)		2	
Mental eminence (1-5)		2	

CT Scan 4	Left	Center	Right
Nuchal crest (1-5)		1	
Mastoid process (1-5)	2		1
Supraorbital margin (1-5)	2		1
Glabella (1-5)		2	
Mental eminence (1-5)		1	

Dry Skull 5	Left	Center	Right
Nuchal crest (1-5)		4	
Mastoid process (1-5)	4		3
Supraorbital margin (1-5)	2		2
Glabella (1-5)		5	
Mental eminence (1-5)		4	

CT Scan 5	Left	Center	Right
Nuchal crest (1-5)		4	
Mastoid process (1-5)	4		3
Supraorbital margin (1-5)	2		2
Glabella (1-5)		5	
Mental eminence (1-5)		4	

Dry Skull 6	Left	Center	Right
Nuchal crest (1-5)		1	
Mastoid process (1-5)	1		1
Supraorbital margin (1-5)	2		2
Glabella (1-5)		2	
Mental eminence (1-5)		2	

CT Scan 6	Left	Center	Right
Nuchal crest (1-5)		1	
Mastoid process (1-5)	1		1
Supraorbital margin (1-5)	3		3
Glabella (1-5)		2	
Mental eminence (1-5)		2	

Dry Skull 7	Left	Center	Right
Nuchal crest (1-5)		5	
Mastoid process (1-5)	3		3
Supraorbital margin (1-5)	4		4
Glabella (1-5)		5	
Mental eminence (1-5)		5	

CT Scan 7	Left	Center	Right
Nuchal crest (1-5)		5	
Mastoid process (1-5)	3		3
Supraorbital margin (1-5)	4		3
Glabella (1-5)		5	
Mental eminence (1-5)		5	

Dry Skull 8	Left	Center	Right
Nuchal crest (1-5)		1	
Mastoid process (1-5)	2		2
Supraorbital margin (1-5)	1		1
Glabella (1-5)		1	
Mental eminence (1-5)		2	

CT Scan 8	Left	Center	Right
Nuchal crest (1-5)		1	
Mastoid process (1-5)	3		2
Supraorbital margin (1-5)	1		1
Glabella (1-5)		1	
Mental eminence (1-5)		2	

Figure 4.1. Scoring results following Walker (2008) and Buikstra and Ubelaker (1994).

For each of these morphological traits, percent agreement of scores between the dry skull and the CT sample was calculated. The nuchal crest scores yielded 100% agreement, the mastoid process scores yielded 68.8% agreement, the supraorbital margin scores yielded 62.5% agreement, the glabella scores yielded 87.5% agreement, and the mental eminence scores yielded 75.0% agreement. For each individual difference between dry skull and CT scan scores, deviation was never greater than +/- 1 ordinal score.

Table 4.1. Logistic discriminant analysis equations for sex estimation from Walker (2008: 47).

Population-specific discriminate functions[a]	% Classified correctly: Males	% Classified correctly: Females	% Sex bias[b]
American/English			
Y = glabella × −1.375 + mastoid × −1.185 + mental × −1.151 + 9.128	88.4	86.4	2.0
Y = glabella × −1.568 + mastoid × −1.459 + 7.434	85.4	82.9	2.5
Y = glabella × −1.525 + mental × −1.485 + 7.372	86.6	82.1	4.5
Y = mental × −1.629 + mastoid × −1.415 + 7.382	79.9	83.6	−3.7
Y = orbit × −1.007 + mental × −1.850 + 6.018	78.1	77.9	0.2
Y = nuchal × −0.7 + mastoid × −1.559 + 5.329	76.8	82.9	−6.1
Native American			
Y = orbit × −0.499 + mental × −0.606 + 3.414	78.1	77.9	0.2
Y = mental × −0.576 + mastoid × −1.136 + 4.765	74.1	72.7	1.4
Y = glabella × −0.797 + mastoid × −1.085 + 5.025	69.5	82.9	−13.4

[a] These models were selected so that the equations only include statistical significance coefficients; significant effects are suggested when confidence intervals do not contain 0. The value of y is a discriminant function score in which the cut point between males and females is 0. Skulls with values of > 0 are more likely to be females and skulls with scores of < 0 are more likely to be males.
[b] % Sex bias = (% males correctly classified − % female correctly classified).

The scores for each dry skull and CT scan were entered into Walker's (2008) first logistic discriminant analysis equation for the American/English population (Table 4.1) which utilizes the scores for glabella, mastoid process, and mental eminence and has the highest correct classification percentage out of all the equations available. The resulting sex estimations not only were consistent for each dry skull-to-CT scan pairing, but the actual sex of each individual was accurately estimated (Table 4.2).

Table 4.2. Morphological sex estimation using discriminant function equations from Walker (2008).				
	Actual Sex	**Classified as**	**Equation used**	**Y-value**
Skull 1	Male	Male	Y = glabella(4) x -1.375 + mastoid(4) x -1.185 + mental(3) x -1.151 + 9.128	-4.565
CT 1	Male	Male	Y = glabella(4) x -1.375 + mastoid(4) x -1.185 + mental(4) x -1.151 + 9.128	-5.716
Skull 2	Female	Female	Y = glabella(1) x -1.375 + mastoid(2) x -1.185 + mental(2) x -1.151 + 9.128	3.081
CT 2	Female	Female	Y = glabella(2) x -1.375 + mastoid(3) x -1.185 + mental(2) x -1.151 + 9.128	0.521
Skull 3	Male	Male	Y = glabella(4) x -1.375 + mastoid(3) x -1.185 + mental(5) x -1.151 + 9.128	-5.682
CT 3	Male	Male	Y = glabella(4) x -1.375 + mastoid(3) x -1.185 + mental(5) x -1.151 + 9.128	-5.682
Skull 4	Female	Female	Y = glabella(2) x -1.375 + mastoid(1) x -1.185 + mental(2) x -1.151 + 9.128	2.891
CT 4	Female	Female	Y = glabella(2) x -1.375 + mastoid(2) x -1.185 + mental(1) x -1.151 + 9.128	2.857
Skull 5	Male	Male	Y = glabella(5) x -1.375 + mastoid(4) x -1.185 + mental(4) x -1.151 + 9.128	-7.091
CT 5	Male	Male	Y = glabella(5) x -1.375 + mastoid(4) x -1.185 + mental(4) x -1.151 + 9.128	-7.091
Skull 6	Female	Female	Y = glabella(2) x -1.375 + mastoid(1) x -1.185 + mental(2) x -1.151 + 9.128	2.891
CT 6	Female	Female	Y = glabella(2) x -1.375 + mastoid(1) x -1.185 + mental(2) x -1.151 + 9.128	2.891
Skull 7	Male	Male	Y = glabella(5) x -1.375 + mastoid(3) x -1.185 + mental(5) x -1.151 + 9.128	-7.057
CT 7	Male	Male	Y = glabella(5) x -1.375 + mastoid(3) x -1.185 + mental(5) x -1.151 + 9.128	-7.057
Skull 8	Female	Female	Y = glabella(1) x -1.375 + mastoid(2) x -1.185 + mental(2) x -1.151 + 9.128	3.081
CT 8	Female	Female	Y = glabella(1) x -1.375 + mastoid(3) x -1.185 + mental(2) x -1.151 + 9.128	1.896

Evidently, morphological sex estimation using Buikstra and Ubelaker’s (1994) scoring system and Walker’s (2008) logistic discriminant analysis equations is quite accurate when applied to CT scans. The percentage agreements for each individual cranial morphological trait are high, and even when there is deviation it is within one score. Although the Y-values were not identical for dry skull and CT scan pairs 1, 2, 4, and 8, the results of the overall sex estimation using logistic discriminant analysis equations were 100% in agreement overall.

4.2 Morphological Ancestry Estimation Results

Resulting charts from morphological estimation of ancestry using Hefner and Ousley’s (2014) OSSA method are included in Figures 4.2-4.9. This method was not as successful on the CT scan sample as it was on the dry skull sample. Due to poor CT scan resolution around the nasal area, several traits could not be scored, and since the summed OSSA score used to estimate overall ancestry depends on all trait scores, ancestry estimation was not possible for 7/8 of the CT scans.

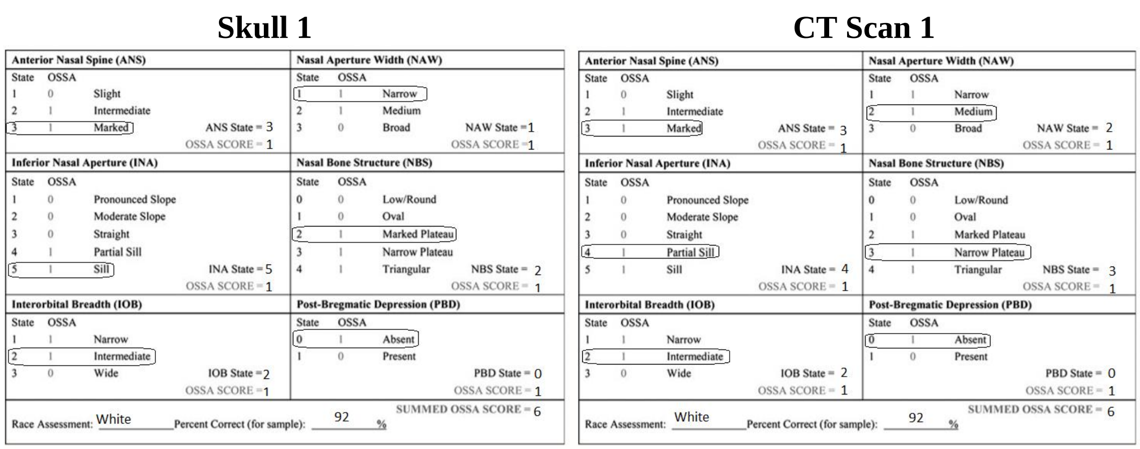

Figure 4.2. OSSA scores for Skull 1 and CT Scan 1 using chart in Hefner and Ousley (2014:4).

Skull 2

State	OSSA	Anterior Nasal Spine (ANS)
1	0	Slight
2	1	Intermediate
3	1	Marked
		ANS State = 3
		OSSA SCORE = 1

State	OSSA	Nasal Aperture Width (NAW)
1	1	Narrow
2	1	Medium
3	0	Broad
		NAW State = 2
		OSSA SCORE = 1

State	OSSA	Inferior Nasal Aperture (INA)
1	0	Pronounced Slope
2	0	Moderate Slope
3	0	Straight
4	1	Partial Sill
5	1	Sill
		INA State = 4
		OSSA SCORE = 1

State	OSSA	Nasal Bone Structure (NBS)
0	0	Low/Round
1	0	Oval
2	1	Marked Plateau
3	1	Narrow Plateau
4	1	Triangular
		NBS State = 3
		OSSA SCORE = 1

State	OSSA	Interorbital Breadth (IOB)
1	1	Narrow
2	1	Intermediate
3	0	Wide
		IOB State = 1
		OSSA SCORE = 1

State	OSSA	Post-Bregmatic Depression (PBD)
0	1	Absent
1	0	Present
		PBD State = 0
		OSSA SCORE = 1

Race Assessment: White Percent Correct (for sample): 92 % SUMMED OSSA SCORE = 6

CT Scan 2

State	OSSA	Anterior Nasal Spine (ANS)
1	0	Slight
2	1	Intermediate
3	1	Marked
		ANS State = 2
		OSSA SCORE = 1

State	OSSA	Nasal Aperture Width (NAW)
1	1	Narrow
2	1	Medium
3	0	Broad
		NAW State = 2
		OSSA SCORE = 1

State	OSSA	Inferior Nasal Aperture (INA)
1	0	Pronounced Slope
2	0	Moderate Slope
3	0	Straight CANNOT SCORE
4	1	Partial Sill
5	1	Sill
		INA State =
		OSSA SCORE =

State	OSSA	Nasal Bone Structure (NBS)
0	0	Low/Round
1	0	Oval
2	1	Marked Plateau
3	1	Narrow Plateau
4	1	Triangular
		NBS State = 2
		OSSA SCORE = 1

State	OSSA	Interorbital Breadth (IOB)
1	1	Narrow
2	1	Intermediate
3	0	Wide
		IOB State = 1
		OSSA SCORE = 1

State	OSSA	Post-Bregmatic Depression (PBD)
0	1	Absent
1	0	Present
		PBD State = 0
		OSSA SCORE = 1

Race Assessment: N/A Percent Correct (for sample): N/A % SUMMED OSSA SCORE = N/A

Figure 4.3. OSSA scores for Skull 2 and CT Scan 2 using chart in Hefner and Ousley (2014:4).

Skull 3

State	OSSA	Anterior Nasal Spine (ANS)
1	0	Slight
2	1	Intermediate
3	1	Marked
		ANS State = 3
		OSSA SCORE = 1

State	OSSA	Nasal Aperture Width (NAW)
1	1	Narrow
2	1	Medium
3	0	Broad
		NAW State = 1
		OSSA SCORE = 1

State	OSSA	Inferior Nasal Aperture (INA)
1	0	Pronounced Slope
2	0	Moderate Slope
3	0	Straight
4	1	Partial Sill
5	1	Sill
		INA State = 4
		OSSA SCORE = 1

State	OSSA	Nasal Bone Structure (NBS)
0	0	Low/Round
1	0	Oval
2	1	Marked Plateau
3	1	Narrow Plateau
4	1	Triangular
		NBS State = 2
		OSSA SCORE = 1

State	OSSA	Interorbital Breadth (IOB)
1	1	Narrow
2	1	Intermediate
3	0	Wide
		IOB State = 2
		OSSA SCORE = 1

State	OSSA	Post-Bregmatic Depression (PBD)
0	1	Absent
1	0	Present
		PBD State = 0
		OSSA SCORE = 1

Race Assessment: White Percent Correct (for sample): 92 % SUMMED OSSA SCORE = 6

CT Scan 3

State	OSSA	Anterior Nasal Spine (ANS)
1	0	Slight
2	1	Intermediate
3	1	Marked
		ANS State = 2
		OSSA SCORE = 1

State	OSSA	Nasal Aperture Width (NAW)
1	1	Narrow
2	1	Medium
3	0	Broad
		NAW State = 1
		OSSA SCORE = 1

State	OSSA	Inferior Nasal Aperture (INA)
1	0	Pronounced Slope
2	0	Moderate Slope CANNOT SCORE
3	0	Straight
4	1	Partial Sill
5	1	Sill
		INA State =
		OSSA SCORE =

State	OSSA	Nasal Bone Structure (NBS)
0	0	Low/Round
1	0	Oval
2	1	Marked Plateau
3	1	Narrow Plateau
4	1	Triangular
		NBS State = 2
		OSSA SCORE = 1

State	OSSA	Interorbital Breadth (IOB)
1	1	Narrow
2	1	Intermediate
3	0	Wide
		IOB State = 1
		OSSA SCORE = 1

State	OSSA	Post-Bregmatic Depression (PBD)
0	1	Absent
1	0	Present
		PBD State = 0
		OSSA SCORE = 1

Race Assessment: N/A Percent Correct (for sample): N/A % SUMMED OSSA SCORE = N/A

Figure 4.4. OSSA scores for Skull 3 and CT Scan 3 using chart in Hefner and Ousley (2014:4).

Skull 4

Anterior Nasal Spine (ANS) State	OSSA		Nasal Aperture Width (NAW) State	OSSA	
1	0	Slight	1	1	Narrow
2	1	Intermediate	2	1	Medium
3	1	Marked	3	0	Broad
		ANS State = 3, OSSA SCORE = 1			NAW State = 1, OSSA SCORE = 1

Inferior Nasal Aperture (INA) State	OSSA		Nasal Bone Structure (NBS) State	OSSA	
1	0	Pronounced Slope	0	0	Low/Round
2	0	Moderate Slope	1	0	Oval
3	0	Straight	2	1	Marked Plateau
4	1	Partial Sill	3	1	Narrow Plateau
5	1	Sill	4	1	Triangular
		INA State = 4, OSSA SCORE = 1			NBS State = 2, OSSA SCORE = 1

Interorbital Breadth (IOB) State	OSSA		Post-Bregmatic Depression (PBD) State	OSSA	
1	1	Narrow	0	1	Absent
2	1	Intermediate	1	0	Present
3	0	Wide			
		IOB State = 1, OSSA SCORE = 1			PBD State = 1, OSSA SCORE = 0

Race Assessment: White Percent Correct (for sample): 94 % SUMMED OSSA SCORE = 5

CT Scan 4

Anterior Nasal Spine (ANS) State	OSSA		Nasal Aperture Width (NAW) State	OSSA	
1	0	Slight CANNOT SCORE	1	1	Narrow
2	1	Intermediate	2	1	Medium
3	1	Marked	3	0	Broad
		ANS State = , OSSA SCORE =			NAW State = 2, OSSA SCORE = 1

Inferior Nasal Aperture (INA) State	OSSA		Nasal Bone Structure (NBS) State	OSSA	
1	0	Pronounced Slope	0	0	Low/Round
2	0	Moderate Slope	1	0	Oval
3	0	Straight CANNOT SCORE	2	1	Marked Plateau
4	1	Partial Sill	3	1	Narrow Plateau
5	1	Sill	4	1	Triangular
		INA State = , OSSA SCORE =			NBS State = 2, OSSA SCORE = 1

Interorbital Breadth (IOB) State	OSSA		Post-Bregmatic Depression (PBD) State	OSSA	
1	1	Narrow	0	1	Absent
2	1	Intermediate	1	0	Present
3	0	Wide			
		IOB State = 1, OSSA SCORE = 1			PBD State = 1, OSSA SCORE = 0

Race Assessment: N/A Percent Correct (for sample): N/A % SUMMED OSSA SCORE = N/A

Figure 4.5. OSSA scores for Skull 4 and CT Scan 4 using chart in Hefner and Ousley (2014:4).

Skull 5

Anterior Nasal Spine (ANS) State	OSSA		Nasal Aperture Width (NAW) State	OSSA	
1	0	Slight	1	1	Narrow
2	1	Intermediate	2	1	Medium
3	1	Marked	3	0	Broad
		ANS State = 3, OSSA SCORE = 1			NAW State = 2, OSSA SCORE = 1

Inferior Nasal Aperture (INA) State	OSSA		Nasal Bone Structure (NBS) State	OSSA	
1	0	Pronounced Slope	0	0	Low/Round
2	0	Moderate Slope	1	0	Oval
3	0	Straight	2	1	Marked Plateau
4	1	Partial Sill	3	1	Narrow Plateau
5	1	Sill	4	1	Triangular
		INA State = 4, OSSA SCORE = 1			NBS State = 2, OSSA SCORE = 1

Interorbital Breadth (IOB) State	OSSA		Post-Bregmatic Depression (PBD) State	OSSA	
1	1	Narrow	0	1	Absent
2	1	Intermediate	1	0	Present
3	0	Wide			
		IOB State = 2, OSSA SCORE = 1			PBD State = 0, OSSA SCORE = 1

Race Assessment: White Percent Correct (for sample): 92 % SUMMED OSSA SCORE = 6

CT Scan 5

Anterior Nasal Spine (ANS) State	OSSA		Nasal Aperture Width (NAW) State	OSSA	
1	0	Slight	1	1	Narrow
2	1	Intermediate	2	1	Medium
3	1	Marked	3	0	Broad
		ANS State = 3, OSSA SCORE = 1			NAW State = 2, OSSA SCORE = 1

Inferior Nasal Aperture (INA) State	OSSA		Nasal Bone Structure (NBS) State	OSSA	
1	0	Pronounced Slope	0	0	Low/Round
2	0	Moderate Slope	1	0	Oval
3	0	Straight CANNOT SCORE	2	1	Marked Plateau
4	1	Partial Sill	3	1	Narrow Plateau
5	1	Sill	4	1	Triangular
		INA State = , OSSA SCORE =			NBS State = 2, OSSA SCORE = 1

Interorbital Breadth (IOB) State	OSSA		Post-Bregmatic Depression (PBD) State	OSSA	
1	1	Narrow	0	1	Absent
2	1	Intermediate	1	0	Present
3	0	Wide			
		IOB State = 1, OSSA SCORE = 1			PBD State = 0, OSSA SCORE = 1

Race Assessment: N/A Percent Correct (for sample): N/A % SUMMED OSSA SCORE = N/A

Figure 4.6. OSSA scores for Skull 5 and CT Scan 5 using chart in Hefner and Ousley (2014:4).

Skull 6

Anterior Nasal Spine (ANS)			Nasal Aperture Width (NAW)		
State	OSSA		State	OSSA	
1	0	Slight	1	1	Narrow
2	1	Intermediate	2	1	Medium
3	1	Marked	3	0	Broad
		ANS State = 2			NAW State = 1
		OSSA SCORE = 1			OSSA SCORE = 1
Inferior Nasal Aperture (INA)			**Nasal Bone Structure (NBS)**		
State	OSSA		State	OSSA	
1	0	Pronounced Slope	0	0	Low/Round
2	0	Moderate Slope	1	0	Oval
3	0	Straight	2	1	Marked Plateau
4	1	Partial Sill	3	1	Narrow Plateau
5	1	Sill	4	1	Triangular
		INA State = 5			NBS State = 4
		OSSA SCORE = 1			OSSA SCORE = 1
Interorbital Breadth (IOB)			**Post-Bregmatic Depression (PBD)**		
State	OSSA		State	OSSA	
1	1	Narrow	0	1	Absent
2	1	Intermediate	1	0	Present
3	0	Wide			
		IOB State =2			PBD State = 0
		OSSA SCORE =1			OSSA SCORE = 1
Race Assessment: White		Percent Correct (for sample): 92 %			SUMMED OSSA SCORE = 6

CT Scan 6

Anterior Nasal Spine (ANS)			Nasal Aperture Width (NAW)		
State	OSSA		State	OSSA	
1	0	Slight CANNOT SCORE	1	1	Narrow
2	1	Intermediate	2	1	Medium
3	1	Marked	3	0	Broad
		ANS State =			NAW State = 2
		OSSA SCORE =			OSSA SCORE = 1
Inferior Nasal Aperture (INA)			**Nasal Bone Structure (NBS)**		
State	OSSA		State	OSSA	
1	0	Pronounced Slope	0	0	Low/Round
2	0	Moderate Slope	1	0	Oval
3	0	Straight CANNOT SCORE	2	1	Marked Plateau
4	1	Partial Sill	3	1	Narrow Plateau
5	1	Sill	4	1	Triangular
		INA State =			NBS State = 4
		OSSA SCORE =			OSSA SCORE = 1
Interorbital Breadth (IOB)			**Post-Bregmatic Depression (PBD)**		
State	OSSA		State	OSSA	
1	1	Narrow	0	1	Absent
2	1	Intermediate	1	0	Present
3	0	Wide			
		IOB State = 2			PBD State = 0
		OSSA SCORE = 1			OSSA SCORE = 1
Race Assessment: N/A		Percent Correct (for sample): N/A %			SUMMED OSSA SCORE = N/A

Figure 4.7. OSSA scores for Skull 6 and CT Scan 6 using chart in Hefner and Ousley (2014:4).

Skull 7

Anterior Nasal Spine (ANS)			Nasal Aperture Width (NAW)		
State	OSSA		State	OSSA	
1	0	Slight	1	1	Narrow
2	1	Intermediate	2	1	Medium
3	1	Marked	3	0	Broad
		ANS State = 2			NAW State = 2
		OSSA SCORE = 1			OSSA SCORE = 1
Inferior Nasal Aperture (INA)			**Nasal Bone Structure (NBS)**		
State	OSSA		State	OSSA	
1	0	Pronounced Slope	0	0	Low/Round
2	0	Moderate Slope	1	0	Oval
3	0	Straight	2	1	Marked Plateau
4	1	Partial Sill	3	1	Narrow Plateau
5	1	Sill	4	1	Triangular
		INA State = 5			NBS State = 3
		OSSA SCORE = 1			OSSA SCORE = 1
Interorbital Breadth (IOB)			**Post-Bregmatic Depression (PBD)**		
State	OSSA		State	OSSA	
1	1	Narrow	0	1	Absent
2	1	Intermediate	1	0	Present
3	0	Wide			
		IOB State = 2			PBD State = 0
		OSSA SCORE = 1			OSSA SCORE = 1
Race Assessment: White		Percent Correct (for sample): 92 %			SUMMED OSSA SCORE = 6

CT Scan 7

Anterior Nasal Spine (ANS)			Nasal Aperture Width (NAW)		
State	OSSA		State	OSSA	
1	0	Slight	1	1	Narrow
2	1	Intermediate	2	1	Medium
3	1	Marked	3	0	Broad
		ANS State = 2			NAW State = 2
		OSSA SCORE = 1			OSSA SCORE = 1
Inferior Nasal Aperture (INA)			**Nasal Bone Structure (NBS)**		
State	OSSA		State	OSSA	
1	0	Pronounced Slope	0	0	Low/Round
2	0	Moderate Slope	1	0	Oval
3	0	Straight CANNOT SCORE	2	1	Marked Plateau
4	1	Partial Sill	3	1	Narrow Plateau
5	1	Sill	4	1	Triangular
		INA State =			NBS State = 3
		OSSA SCORE =			OSSA SCORE = 1
Interorbital Breadth (IOB)			**Post-Bregmatic Depression (PBD)**		
State	OSSA		State	OSSA	
1	1	Narrow	0	1	Absent
2	1	Intermediate	1	0	Present
3	0	Wide			
		IOB State = 1			PBD State = 0
		OSSA SCORE = 1			OSSA SCORE = 1
Race Assessment: N/A		Percent Correct (for sample): N/A %			SUMMED OSSA SCORE = N/A

Figure 4.8. OSSA scores for Skull 7 and CT Scan 7 using chart in Hefner and Ousley (2014:4).

Skull 8 **CT Scan 8**

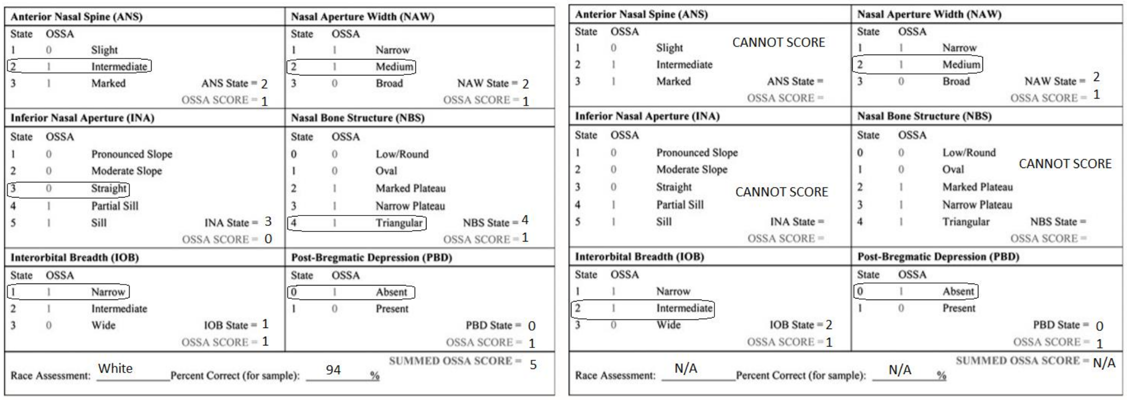

Skull 8

Anterior Nasal Spine (ANS)
State OSSA
1 0 Slight
2 1 Intermediate
3 1 Marked
ANS State = 2
OSSA SCORE = 1

Nasal Aperture Width (NAW)
State OSSA
1 1 Narrow
2 1 Medium
3 0 Broad
NAW State = 2
OSSA SCORE = 1

Inferior Nasal Aperture (INA)
State OSSA
1 0 Pronounced Slope
2 0 Moderate Slope
3 0 Straight
4 1 Partial Sill
5 1 Sill
INA State = 3
OSSA SCORE = 0

Nasal Bone Structure (NBS)
State OSSA
0 0 Low/Round
1 0 Oval
2 1 Marked Plateau
3 1 Narrow Plateau
4 1 Triangular
NBS State = 4
OSSA SCORE = 1

Interorbital Breadth (IOB)
State OSSA
1 1 Narrow
2 1 Intermediate
3 0 Wide
IOB State = 1
OSSA SCORE = 1

Post-Bregmatic Depression (PBD)
State OSSA
0 1 Absent
1 0 Present
PBD State = 0
OSSA SCORE = 1

Race Assessment: White Percent Correct (for sample): 94 %
SUMMED OSSA SCORE = 5

CT Scan 8

Anterior Nasal Spine (ANS)
State OSSA
1 0 Slight
2 1 Intermediate
3 1 Marked
CANNOT SCORE
ANS State =
OSSA SCORE =

Nasal Aperture Width (NAW)
State OSSA
1 1 Narrow
2 1 Medium
3 0 Broad
NAW State = 2
OSSA SCORE = 1

Inferior Nasal Aperture (INA)
State OSSA
1 0 Pronounced Slope
2 0 Moderate Slope
3 0 Straight
4 1 Partial Sill
5 1 Sill
CANNOT SCORE
INA State =
OSSA SCORE =

Nasal Bone Structure (NBS)
State OSSA
0 0 Low/Round
1 0 Oval
2 1 Marked Plateau
3 1 Narrow Plateau
4 1 Triangular
CANNOT SCORE
NBS State =
OSSA SCORE =

Interorbital Breadth (IOB)
State OSSA
1 1 Narrow
2 1 Intermediate
3 0 Wide
IOB State = 2
OSSA SCORE = 1

Post-Bregmatic Depression (PBD)
State OSSA
0 1 Absent
1 0 Present
PBD State = 0
OSSA SCORE = 1

Race Assessment: N/A Percent Correct (for sample): N/A %
SUMMED OSSA SCORE = N/A

Figure 4.9. OSSA scores for Skull 8 and CT Scan 8 using chart in Hefner and Ousley (2014:4).

The resulting ancestry estimations for skulls 1-8 and CT scan 1 were White, with between 92% and 94% accuracy. While there was agreement in the summed OSSA score and overall ancestry estimation for dry skull and CT scan pair 1, the inability to properly conduct ancestry estimation using the OSSA method on the other CT scans leaves total comparison inconclusive at best. However, each of the traits that were able to be scored on the CT scans (with the exception of the post-bregmatic depression score on CT scan 1) had OSSA scores of 1, indicating that if full analysis was possible, it is likely the results would be an estimation of White.

For each of the individual traits, a calculation of percent agreement of scores between the dry skull and the CT samples were determined. This was difficult as well, since many of the traits were not able to be scored. The anterior nasal spine was unable to be scored on CT scans 4, 6, and 8; the inferior nasal aperture was unable to be scored on CT scans 2, 3, 4, 5, 6, 7, and 8; and the nasal bone shape was unable to be scored on CT scan 8. Out of those able to be scored and compared, the anterior nasal spine was scored inconsistently on dry skull and CT scan pairings 2 and 3 and in agreement on pairs 1, 5, and 7; the inferior nasal aperture was scored inconsistently on dry skull and CT scan pair 1 (the only pairing able to be scored); the interorbital breadth was 50% in agreement, being scored inconsistently on dry skull and CT scan pairings 3, 5, 7 and 8 and in agreement on pairs 1, 2, 4 and 7; the nasal aperture width was 62.5% in agreement, being scored inconsistently on dry skull and CT scan pairings 1, 4 and 6 and in agreement on pairs 2, 3, 5, 7 and 8; the nasal bone shape was scored inconsistently on dry skull and CT scan pairings 1 and 2 and in agreement on pairs 3, 4, 5, 6 and 7; and the post-bregmatic depression was 100% in agreement for all pairings. All deviations in character state scores were within one value, and the OSSA score was the same for each deviated score in all cases.

4.3 Statistical Analysis of Measurements

The dry skull and CT scan measurements are detailed in Tables 4.3 and 4.4, respectively. For bilateral measurements, left and right measurements were taken and are included in the tables, although for statistical analysis and FORDISC 3.1 and one-way ANOVA analysis only the left measurement was used, per standard osteometric practice.

Table 4.3. Dry skull measurements.

Measure-ment	Instru-ment	Skull 1		Skull 2		Skull 3		Skull 4		Skull 5		Skull 6		Skull 7		Skull 8	
		L	R	L	R	L	R	L	R	L	R	L	R	L	R	L	R
GOL	Sp.	184		177		192		168		191		174		187		182	
XCB	Sp.	142		142		138		141		144		133		137		141	
ZYB	Sl.	133		125		128		120		136		122		126		123	
AUB	Sp.	123		119		118		118		129		111		118		120	
WFB	Sl.	96		88		88		93		104		87		99		95	
UFBR	Sl.	113		122		104		97		111		102		107		104	
ASB	Sl.	118		114		114		111		116		120		110		109	
NLH	Sl.	51		48		54		50		53		48		48		50	
OBB	Sl.	43	43	38	38	41	40	40	41	41	41	41	41	41	41	40	40
OBH	Sl.	36	35	31	30	33	32	34	34	34	34	35	35	34	33	41	40
EKB	Sl.	104		90		97		93		102		93		99		95	
DKB	Sl.	21		19		24		16		25		17		21		16	
FRC	Sl.	119		111		112		106		117		102		123		113	
PAC	Sl.	118		121		120		108		115		102		124		118	
OCC	Sl.	101		95		102		92		108		97		100		102	
FOL	Sl.	37		38		35		33		35		36		35		36	
FOB	Sl.	30		31		31		27		31		27		30		31	
MDH	Sl.	37	36	33	31	30	33	31	29	33	33	28	27	33	35	33	33
GOG	Sl.	99		89		97		92		99		87		100		92	
WRB	Sl.	35	34	29	29	34	35	24	23	30	29	26	26	30	30	28	29
MLN	Mb.	84		76		80		73		82		68		76		76	
MAN	Mb.	117		125		119		147		134		131		133		135	

Table 4.4. CT scan measurements.

Measurement	Skull 1		Skull 2		Skull 3		Skull 4		Skull 5		Skull 6		Skull 7		Skull 8	
	L	R	L	R	L	R	L	R	L	R	L	R	L	R	L	R
GOL	185		178		192		169		196		175		191		181	
XCB	142		141		137		141		145		132		138		140	
ZYB	135		127		127		116		132		119		127		123	
AUB	125		124		118		116		125		108		118		120	
WFB	96		96		88		92		104		87		99		95	
UFBR	114		99		103		97		112		102		107		102	
ASB	118		116		113		106		113		117		113		112	
NLH	51		51		53		50		52		51		51		51	
OBB	41	40	37	37	40	39	39	39	40	39	40	40	42	42	40	38
OBH	35	35	31	32	35	35	36	35	34	34	36	-	36	36	36	37
EKB	102		92		98		93		100		96		101		95	
DKB	22		17		21		17		22		17		18		18	
FRC	118		112		112		104		116		101		123		106	
PAC	120		121		119		111		123		114		133		131	
OCC	98		93		98		91		105		86		98		100	
FOL	37		38		35		33		35		36		35		36	
FOB	30		33		31		27		31		27		31		32	
MDH	36	36	35	32	30	34	30	29	33	35	28	26	35	36	32	32
GOG	102		89		99		93		100		87		100		92	
WRB	35	35	29	28	33	33	23	23	29	28	24	26	31	30	28	28
MLN	89		85		85		77		92		77		84		79	
MAN	120		131		131		145		129		125		132		132	

Each set of CT and skull measurements was analyzed using a one-way ANOVA (Table 4.5). Results with a *p*-value of 0.05 or lower were considered statistically significant. Every measurement analyzed had a *p*-value of greater than 0.05 except for mandibular length (MLN), meaning that the difference in measurement between the CT and skull measurements is not significant and therefore suggest that measurements made using CT scans can be used in place of measurements taken on dry skulls.

Table 4.5. One-way ANOVA results for each measurement.

Measurement	F-value	Sig. (p-value)
ASB	0.084	0.776
AUB	0.038	0.848
DKB	0.503	0.492
EKB	0.182	0.677
FOB	0.250	0.626
FOL	-1.55431E-15	1
FRC	0.137	0.718
GOG	0.042	0.841
GOL	0.095	0.763
MAN	0.209	0.655
MDH	0.052	0.824
MLN	6.533	0.025
NLH	1.297	0.277
OBB	0.658	0.433
OBH	0.044	0.838
OCC	1.318	0.273
PAC	2.169	0.167
UFBR	1.003	0.336
WFB	0.091	0.769
WRB	0.099	0.758
XCB	0.019	0.893
ZYB	0.201	0.662

Minimum, maximum, and mean (average) deviations were also noted (Table 4.6). This table shows that the majority of the measurements (77.27%) had an average deviation of less than two millimeters (positive or negative), excluding mandibular angle, mandibular length, occipital chord, parietal chord, and upper facial breadth When taking skeletal measurements, deviation of two millimeters or less is considered acceptable when peer reviewing others' measurements (Tallman; pers. comm.).

Table 4.6. Minimum, maximum, and mean deviations for each measurement.

Measurement	Min. Deviation	Max. Deviation	Mean Deviation
ASB	-3	5	0.5
AUB	-5	4	0.25
DKB	-2	3	0.875
EKB	-3	2	-0.5
FOB	-2	0	-0.5
FOL	0	0	0
FRC	-1	7	1.375
GOG	-3	0	-0.875
GOL	-5	1	-1.5
MAN	-25	6	-2.125
MDH	-2	1	-0.125
MLN	-10	-3	-6.625
NLH	-3	1	-1
OBB	-1	2	0.75
OBH	-2	5	-0.125
OCC	1	11	3.5
PAC	-13	1	-5.75
UFBR	-1	23	3
WFB	-8	1	-0.875
WRB	-1	2	0.5
XCB	-1	1	0.25
ZYB	-2	4	0.875

4.4 FORDISC 3.1 Sex and Ancestry Estimation Results

The measurements from each skull that were entered into FORDISC 3.1 and compared against all population groups, which yielded initial results as seen in Table 4.7. All skull-CT pairings were classified into the same overall sex, although the Distance, Posterior probabilities, Type F, and Type Chi statistics were not identical for each pairing. Regardless of the slight statistical differences, sex estimation was consistent for 8/8 (100%) of the sample. However, for dry skull and CT scan pairing 2, the FORDISC 3.1 classification was not correct, classifying the individual as male when correct classification is female.

Table 4.7. FORDISC 3.1 statistics for sex estimation.

	Actual Sex	Classified as	Distance from	Posterior	Type F	Type Chi
Skull 1	Male	Male	12.4	0.663	0.736	0.715
CT 1	Male	Male	8.5	0.409	0.939	0.932
Skull 2	Female	Male	13.6	0.519	0.642	0.630
CT 2	Female	Male	21.8	0.308	0.162	0.151
Skull 3	Male	Male	17.4	0.573	0.390	0.361
CT 3	Male	Male	10.1	0.692	0.871	0.859
Skull 4	Female	Female	10.2	0.694	0.865	0.858
CT 4	Female	Female	15.2	0.465	0.526	0.509
Skull 5	Male	Male	8.5	0.571	0.935	0.932
CT 5	Male	Male	11.4	0.713	0.795	0.786
Skull 6	Female	Female	26.6	0.440	0.061	0.046
CT 6	Female	Female	32.9	0.423	0.011	0.008
Skull 7	Male	Male	15.5	0.325	0.519	0.490
CT 7	Male	Male	28.5	0.469	0.035	0.028
Skull 8	Female	Female	23.5	0.586	0.126	0.102
CT 8	Female	Female	19.5	0.465	0.262	0.245

For FORDISC 3.1 ancestry estimation, all dry skull-CT scan pairings were consistent except for Skull 6 and Skull 8 (Table 4.8). For Skull 6, the dry-skull results indicated the individual was likely Hispanic, although the Distance, Type F, and Type Chi statistics were not strong. For the CT scan measurements of Skull 6, the results were closest to Black, although the FORDISC 3.1 software indicated that this result was too dissimilar to all groups to confidently estimate the ancestry at all. The closest group was reported for the purposes of this study, although in an official anthropological report, the ancestry would likely be reported as "indeterminate." Interestingly, the Posterior Probability is not insignificant, but the Distance, Type F, and Type Chi statistics are very weak.

For Skull 8, the dry-bone measurements yielded an ancestry estimation indicating Hispanic, although the Distance, Type F, and Type Chi statistics are quite weak. However, the CT scan measurements of Skull 8 yielded an ancestry result of White, with stronger statistics across the board than those of the dry-bone results.

Table 4.8. FORDISC 3.1 statistics for ancestry estimation.						
ANCESTRY	**Actual Ancestry**	**Classified as**	**Distance from**	**Posterior**	**Type F**	**Type Chi**
Skull 1	White	Black	11.5	0.649	0.796	0.775
CT 1	White	Black	8.0	0.371	0.954	0.948
Skull 2	White	White	13.2	0.589	0.670	0.654
CT 2	White	White	20.6	0.373	0.210	0.193
Skull 3	White	Black	16.4	0.534	0.458	0.424
CT 3	White	Black	9.8	0.741	0.892	0.879
Skull 4	White	White	15.2	0.752	0.627	0.580
CT 4	White	White	22.4	0.461	0.214	0.169
Skull 5	White	White	8.1	0.580	0.949	0.946
CT 5	White	White	10.4	0.748	0.851	0.843
Skull 6	White	Hispanic	35.2	0.468	0.014	0.006
CT 6	White	Black**	38.5	0.643	0.006	0.002
Skull 7	White	Black	14.7	0.457	0.578	0.546
CT 7	White	Black	27.0	0.490	0.053	0.041
Skull 8	White	Hispanic	35.9	0.598	0.012	0.005
CT 8	White	White	21.4	0.904	0.256	0.207
**CT 6 too dissimilar to all groups according to FORDISC 3.1						

The rest of the dry skull-CT scan pairings yielded consistent ancestry estimations. Like the sex estimation data; however, the statistical Distance, Posterior Probabilities, Type F typicalities, and Type Chi typicalities were not identical. The consistencies between the dry skull/CT scan ancestry estimations were in agreement more often than not though, with 6/8 skulls (75%) being classified consistently. However, only dry skull and CT scan pairings 2, 4, and 5, and CT scan 8 were correctly classified by FORDISC 3.1 as White. This means only 3/8 (37.5%) of the pairings and 7/16 (43.75%) of the overall estimations were classified correctly, making the overall results of ancestry estimation using FORDISC 3.1 mostly consistent, but not exceptionally accurate.

4.5 Conclusion

Morphological sex estimation classified 100% of the dry skull and CT scan pairings consistently and correctly. Comparison of morphological ancestry estimation between most of the dry skull and CT scan sample was not possible due to a number of traits that were unable to be scored, but the overall result was that dry skull and CT scan pairing 1 was in agreement, and 100% of the dry skull sample were characterized correctly.

The results of one-way ANOVA and minimum, maximum, and mean deviation statistical analysis of the measurements taken on the skulls and CT scans produced the overall result that the variance between each measurement from the two samples was not statistically significant (except for the mandibular length, which has a statistically significant p-value). The mean deviations of the majority of the measurements were less than two millimeters (with the exception of mandibular angle, mandibular length, occipital chord, parietal chord, and upper facial breadth), meaning the majority were within the acceptable margin of error for forensic anthropology. Therefore, excluding mandibular angle, mandibular length, occipital chord, parietal chord, and upper facial breadth, measurements taken on CT scans should be serviceable in place of conventional dry bone measurements.

FORDISC 3.1 analysis resulted in consistent sex estimation between each pairing, but Skull/CT Scan 1 was misclassified 1 as male. The correct classification for this individual is female. The FORDISC 3.1 ancestry estimation results were neither particularly consistent or correct.

Morphological sex estimation was consistent between the dry skulls and CT scan samples and also classified each individual correctly, while the FORDISC 3.1 metric sex estimation classified each pairing consistently, but misclassified Skull/CT Scan 2. Overall, both methods had 100% consistency between the skull sample and the CT scan sample, and highly accurate sex estimation. The morphological ancestry estimation could only be done on the skull sample and one of the CT scans, so it is difficult to compare the morphological and FORDISC 3.1 results. However, the morphological ancestry estimation classified all the skulls and the one CT scan correctly, and the one pair was in agreement. The FORDISC 3.1 ancestry estimation did not perform well, and due to the majority of the CT scans not being morphologically estimable and the poor metric performance, only three morphological and metric ancestry estimations were consistently and correctly classified as White.

Chapter V: DISCUSSION

5.1 Morphological Analysis

Morphological sex estimation using Buikstra and Ubelaker's (1994) scoring system and Walker's (2008) logistic discriminant analysis equations classified all of the dry skull and CT scan pairings as White, meaning they were both consistent and correctly classified. While not all of the individual traits for sex estimation were identical for each pairing, the overall resulting sex estimation was not affected. These divergent scores were always within one value, a difference that may be explicable by the inability to physically feel the surface of the skull in the CT scan sample, difficulty viewing the traits at all angles in the CT scan viewing software, or simple observer error.

Morphological estimation of ancestry using Hefner and Ousley's (2014) OSSA method was met with more difficulty, due to the necessity of scoring all six traits to produce a usable OSSA score. Scoring was not a problem on the dry skull sample, but due to issues in visibility of the more delicate features in the nasal region on the CT scans, the majority were not able to be fully scored and therefore produced no accurate estimation of ancestry. The skulls and CT scan that could be assessed were correctly classified as White, but any further comparison was impossible and therefore the results were inconclusive. For individual trait comparison, most of the traits scored, even on the CT scans with missing information, had an OSSA score of 1 indicating a feature consistent with a White individual. For the comparison of scored features, performance was not very consistent, with the highest instance of agreement being nasal aperture width at 62.5% agreement. However, each deviation in scoring was within one value, and each had an OSSA score of 1, so even if overall estimation was possible these deviations would not have an effect on the outcome.

5.2 Measurements

The major findings of this study demonstrated that measurements taken on CT scans do not have a statistically significant difference from measurements taken on the actual skulls, with the only exception being the mandibular length. However, this difference may be due to observer error in measuring one or more of the dry mandibles or CT scans of the mandibles, or inability to access the proper angle within the limits of the CT viewing software given the placement of the mandibles relative to the crania on the scanning bed. Although the differences for mandibular angle, occipital chord, parietal chord, and upper facial breadth were not found to be significant, these measurements were found to have higher mean deviations. Despite this, the overall findings show that using CT scans are an effective means for obtaining measurements for determining the sex and ancestry of an unidentified skull.

In this study, most measurements (77.27%) had a mean difference of less than two millimeters between the actual skull and the CT scan, which is the generally accepted margin of error in forensic anthropology (Tallman; pers. comm.) and therefore measurements from skull CT scans can be used in place of dry bone skull measurements with an acceptable margin of error, but mandibular length should be excluded, as well as perhaps mandibular angle, occipital chord, parietal chord, and upper facial breadth due to mean deviations of over two millimeters. Some of the skulls used in the sample do not have very well-defined cranial sutures, which did not show up well on the CT scans, perhaps due to age-related diminished bone mineral density. This could explain the occipital chord and parietal chord disparities. The mandibles were somewhat difficult to visualize from all angles in the CT scans since they were situated behind the crania in order to fit on the CT scan table, so this may explain the deviance of over two millimeters in mandibular length and mandibular angle. Upper facial breadth may have had a mean difference of over two millimeters simply due to observer error; however, another possibility that may explain the mean deviations of these five measurements is that in general, they are larger measurements. This means that even if the mean deviations are over two millimeters on these measurements, the overall effect of being slightly over or under may be less than for smaller measurements.

The results of the measurement comparison section of this study are comparable to the results of other studies testing the same manner of dry bone-CT scan comparison. Results of studies by Stull *et al.* (2014) and Zech *et al.* (2012) indicated that measurements taken using CT scans are generally accurate when compared to the same measurements taken on dry bone, and the current study corroborates those findings.

From a user standpoint, the process of obtaining measurements from the CT scans was relatively easy. The RadiAnt 5.5.1 software was user-friendly and the mechanisms for movement for viewing the volume-rendered CT scans at different angles were simple and effective. The calibration tool to switch measurements from pixels to millimeters was straightforward as well. For scoring the morphological traits, the movement mechanisms were effective, although for some of the traits such as supra-orbital margin and mental eminence, the ability to physically feel the skull's contours is beneficial.

Despite the mean difference being over two millimeters in five measurements, regarding the one-way ANOVA results it appears that skull CT scan and dry bone skull measurements are more or less interchangeable, excluding mandibular length. However, this study does not test intra- or inter-observer error through repeated measurements of the same skull or skulls, so it is not known how far each measurement is from the "correct" measurement. Thus, it is not certain which particular set of measurements is the "correct" one for each skull, and therefore not possible to choose whether measurements derived from CT scans or from dry skulls are more accurate. However, in similar research, intra-observer accuracy was found to be high (Stull *et al.* 2014). What can be said is that statistically, skull measurements and skull CT measurements do not vary significantly and therefore CT scans may be used in lieu of dry bone with reasonable assumption of accuracy.

5.3 FORDISC 3.1 Analysis

FORDISC 3.1 analysis was generally consistent between the dry skull-CT scan datasets, excluding the ancestry estimation for two skull-CT pairings. Overall, the sex estimation was fully consistent between each skull-CT scan pairing, and the ancestry estimation was consistent in the majority (75%) of the pairings. However, the donor individuals' actual ancestries were incorrectly estimated by FORDISC 3.1 for Skulls 1, 3, 6, 7, and 8, and CT scans 1, 3, 6, and 7. The sexes of Skull 2 and CT scan 2 were incorrectly estimated by FORDISC 3.1 as well. Therefore, FORDISC 3.1 analysis appears to be mostly reliable when using cranial CT measurements instead of traditional dry skull measurements; however, the results may not be necessarily accurate.

Although five of the measurements used in this study had an average difference greater than the accepted forensic anthropological variability of two millimeters, this did not appear to affect the FORDISC 3.1 analysis. This could be because three out of five of these measurements (upper facial breadth, mandibular length, and mandibular angle) were automatically removed from sex and ancestry analysis by FORDISC 3.1 discriminant functions, or it could be because even with over two millimeters of difference the CT scan measurements still fell within the same group as the skull measurements.

Other studies examining FORDISC ancestry estimation have also had somewhat poor results. When used on Thai and French individuals of known sex and ancestry, prediction was inaccurate, although slightly better on the French sub-sample (Guyomarc'h and Bruzek 2011). Another study found estimation of ancestry using FORDISC to be correct for a paltry one percent out of 200 individuals (Elliot and Collard 2009). FORDISC has also been noted too often misclassify Hispanic individuals as Japanese. This was found to be likely due to morphological similarities between those two ancestral groups (Dudzik and Jantz 2016). In light of the failures of these previous studies to correctly classify ancestry, the findings in the current study are likely due to FORDISC 3.1 error rather than errors in measurement.

Overall, it appears that FORDISC 3.1 can be used with either CT scan or dry skull measurements to estimate sex, but perhaps should be avoided for ancestry estimation. As with any method of sex or ancestry estimation, the overall result should be based off of FORDISC 3.1 in conjunction with other methods.

5.4 Comparison of Morphological and Metric Methods

The morphological and metric sex estimation methods were nearly consistent, with the only outlier being dry skull and CT scan pairing 2, a female individual which FORDISC 3.1 misclassified as male. Therefore, it appears that according to this small sample, morphological sex estimation methods from Walker (2008) perform better than metric FORDISC analysis on both dry skulls and CT scans. This may be due to the measurements of Skull 2 being slightly larger than typical female dimensions, but still possessing gracile morphological features, or simply due to FORDISC misclassification. Sex estimation using FORDISC, although typically more accurate than ancestry estimation, has been observed to be erroneous in prior research (Guyomarc'h and Bruzek 2011).

Comparison of morphological and metric ancestry estimation is rather impractical, given that only one CT scan could be effectively assessed to produce an overall estimate. However, given the apparent trajectory of the visible traits on the rest of the sample, it appears that the overall scoring would have resulted in ancestry estimations of White for all the CT scans. This, however, is merely conjecture, and no legitimate conclusions can be drawn based on conjecture. Based on this, the comparison of the morphological and metric methods of ancestry estimation remains, for the most part, inconclusive. Nonetheless, for the skulls and CT scan with observable results, morphological methods using Hefner and Ousley (2014) performed much more accurately than FORDISC 3.1.

5.5 Limitations

As with any study, this research study did have limitations. The first limitation was the small sample size of only eight skulls being used, and the circumstances and conditions of the skulls. Since the sample used comes from the Boston University skeletal donor collection, which tends to bias towards older individuals, many of the skulls used are partially or fully lacking in dentition. This made taking many standard cranial and mandibular measurements impossible, thus excluding them from the statistical variance and FORDISC 3.1 analyses which can result in limitations in the discriminant functions applicable for sex and ancestry estimation, and therefore limiting performance. Another factor of older age is decreased bone mineral density, which may have been the cause of poor resolution on many of the CT scans.

FORDISC 3.1 presented its own set of limitations for this study. Although a generally reliable system of sex and ancestry estimation, it is not broad enough to encompass every distinct ancestral variant. For example, if the individual in question was in fact biracial, or if they had a Brazilian ancestral background, these specific categories are not options and therefore the individual would be misclassified as the next “closest” ancestral group. FORDISC 3.1 can only sort the individual into the closest category, even if in reality the individual is none of the above. Also, some of the measurements omitted due to unavailability may have been crucial to accurate estimation of ancestry. However, if a measurement is not able to be taken in the normal fashion, it is generally accepted practice to simply omit it rather than try to estimate what the measurement would be under normal circumstances.

In the CT viewing software, the measurement default was set to pixels, so it was necessary to calibrate the tool to millimeters using a ten-centimeter scale included on the screen. This calibration had to be redone in every different position in which the skull was viewed, and therefore a few pixels of error may have been introduced for each calibration. Given the statistical insignificance of the difference between the skull and CT scan measurements, however, it is unlikely that this calibration error had a large impact on the results.

Another factor that introduced limitations was the use of CT scans on dry, defleshed skulls in this study. CT imaging technology is designed to scan intact bodies rather than dry bones. This study used dry skulls, which are not optimal conditions for clarity and resolution of the CT scans. The resolution of the CT scans had an effect on the visibility of some cranial sutures, therefore making measurements that rely on suture visibility harder to attain and possibly less accurate. These issues with visibility were also likely due to decreased bone density in the older individuals. Also, due to the limited manipulability of the 3D skull images in the digital viewing software, some standard measurements usually used in FORDISC, such as basion-bregma height, basion-nasion length, and basion-prostheon length were not able to be taken. As stated above, visibility also posed an issue when scoring some of the morphological traits.

Chapter VI: CONCLUSIONS

6.1 Viability of CT Scans

CT scans are an accurate scanning modality used in medicine, including for the planning of surgeries and viewing of internal structures of living people. This technology has also been applied to forensics in the form of virtual autopsy and dry bone analysis. Other studies (Stull *et al.* 2014; Zech *et al.* 2012) have confirmed the accuracy of CT scans in the measurement of bone, fleshed and dry, even though the technology was developed on fleshed subjects for use on fleshed subjects. This study, in general, corroborates the findings of previous research, confirming that CT scans can be used effectively on skeletal materials for purposes of morphological and metric analysis.

Morphological traits for sex estimation performed better than metric, and the morphological ancestry estimation, although limited, had more accuracy than metric on the dry skull sample. However, morphological ancestry estimation was only possible on one CT scan. Due to the high instance of success of morphological sex estimation, it is apparent that CT scans can be used just as effectively as dry bone for these purposes. For morphological ancestry estimation, Hefner and Ousley's (2014) OSSA method should only be attempted if the resolution of the CT scan is strong and all traits are clearly visible.

Based on the findings of this study, cranial measurements from CT scans are generally not significantly different than those taken physically on dry bone using calipers. Statistical analysis of the variance between CT measurements and dry bone measurements of the skulls states that the two methods are more or less interchangeable, except the mandibular length. Additional analysis determined that most of the measurements involved had an average difference within the acceptable error in forensic anthropology of two millimeters.

The selected measurements were similar enough to have a high accuracy in estimating the sex of the individuals using FORDISC 3.1, however the discrepancies between measurement methods were significant enough to cause slight differences in the estimation of ancestry using the same program. Therefore, this study concludes that measurements derived from CT scans may be accurate enough to estimate sex using established formulae, but the slight variability between dry bone and CT scan derived measurements makes estimation of ancestry inadvisable without additional methods supporting the FORDISC 3.1 analysis.

Overall, assessment of morphological traits worked slightly better than metric assessment for sex estimation between cranial CT scans and dry skulls. While ancestry estimation produced accurate results in morphological assessment of the dry skull sample, the results of morphological assessment of the CT scan sample, FORDISC 3.1 assessment of the dry skull sample, and FORDISC 3.1 assessment of the CT scan sample were unfavorable. It is therefore recommended that future researchers and caseworkers use caution when estimating ancestry from CT scans, especially when using morphological character states which may be located in thinner areas of the skull or on older individuals, and to avoid FORDISC 3.1 estimation of ancestry when possible. If access to the physical bone is not available, it is evident that sex estimation methods remain quite accurate when conducted on CT scans.

6.2 Implications of the Current Research

The findings of this study seem to be in agreement with previous medical and forensic research. In medical research, studies have found cranial CT scans to be accurate enough to perform measurements for planning craniofacial surgeries (Cavalcanti *et al.* 1999; Waitzman *et al.* 1992a; Waitzman *et al.* 1992b) and building prosthetics for craniofacial surgeries using 3D printed proxies of the skull (Zheng *et al.* 2019). Cavalcanti *et al.* (1999) found no statistically significant difference in measurements of CT scans versus dry skulls, findings that are corroborated in the results of the current research even though the study by Cavalcanti *et al.* used CT scans of fleshed heads rather than dry bone, whereas this study used already defleshed skulls.

This study also confirms the utility of CT scans in forensic work, building on the work of Thali *et al.* (2003), Aghayev *et al.* (2008), Dedouit *et al.* (2007, 2014), Aalders *et al.* (2017), Lo Re *et al.* (2018), Joshi *et al*. (2018), and Carew and Errickson (2019), exploring the practicality of virtopsy. This study provides supplementary affirmation for the utility of CT scans in further forensic anthropological research and casework. Along with research by Colman *et al.* (2019), Christensen *et al.* (2018), Zech *et al.* (2012), and Stull *et al.* (2014), this study provides not only error rates and corroboration of accuracy, but additional considerations in regards to troubleshooting possible issues in CT scan resolution and manipulability. With current and future research on the efficacy of CT scans in forensic anthropological research as well as constant advancement in technology, the issues of diversity in study samples, accessibility to skeletal collections, factors preventing maceration, conducting autopsy on fragile or otherwise compromised remains, and retention of detailed autopsy information (among others), are on their way to being solved.

Regarding estimation of ancestry using FORDISC for both the dry skull and the CT scan samples, the findings of this study are generally in agreement with prior research. Ancestry estimation using FORDISC has been found by many studies to be flawed, often misclassifying remains (Guyomarc'h and Bruzek 2011; Elliot and Collard 2009; Dudzik and Jantz 2016). Due to this, FORDISC analysis of ancestry is perhaps of limited utility, whether conducted routinely on dry skulls or in a novel fashion on CT scans.

The current research builds on the body of literature concerning the use of CT scans, especially in forensic anthropological contexts. The data provided here may provide valuable confirmation that measurements taken using CT scans and morphological analysis in cases with sufficient resolution are highly adequate and provide demonstrable documentation of error, making forensic anthropological CT scan analysis more likely to be accepted in court. The implications of the results may help guide future research practices and casework protocols by emphasizing strengths and weaknesses of the applications of specific forensic anthropological methods on CT scans. The findings of the current study may be pertinent in cautioning researchers to avoid estimating ancestry from CT scans using FORDISC 3.1 and calling attention to the potential for lost information due to poor CT scan resolution.

6.3 Further Directions and Recommendations

In the future, it is recommended that similar studies be undertaken on the rest of the bones in the human body used to estimate biological profile, including the os coxa for sex estimation and the long bones for stature estimation, to name a few. Some such studies exist already (Colman *et al.* 2019; Stull *et al.* 2014; Zech *et al.* 2012); however, in order to be acceptable in court under the legal standards established in *Daubert v. Merrell Dow Pharmaceuticals* (509 U.S. 579 (1993)) the science must be based on reliable, scientifically testable methods and theories, be based on established standards, have a known error rate, be subject to peer review, and be widely accepted in the scientific community; and to be admissible in states which uphold the standard set by *Frye v. United States* (293 F. 1013 (D.C.. Cir 1923)), the science must be generally accepted in the relevant field. As federal court systems and most states have adopted *Daubert,* in most cases there must be known and tested margins of error for any science used in a court setting. Therefore, even though CT scans are widely used in forensic and medical research, further study is warranted to ensure court admissibility, especially the lesser-tested morphological methods.

In addition to more general research on the use of CT scans in identification and biological profile assessment, subsequent research should also be conducted exploring the causes and possible solutions to the resolution and visibility issues in this study. Perhaps comparison studies of CT scans taken from fleshed and dry samples, or an exploration of the differences between medical CT scanning technology and industrial CT scans. Industrial CT scanning equipment was not available for this study, but according to Christensen *et al.* (2018), this technology may be better suited for forensic purposes than medical CT scans.

Further research seems to be needed as well to explore the apparent tendency of FORDISC to misclassify ancestry. This tendency was noted in past studies by Guyomarc'h and Bruzek (2011), Elliot and Collard (2009), and Dudzik and Jantz (2016), and the issues underscored by this previous research were corroborated by the poor performance of FORDISC 3.1 ancestry estimation in the current study. If the current study were to be improved upon in future research, automated analysis of sex using Klales' (2020) MorphoPASSE system would be analyzed, and the skull sample used would omit edentulous individuals or those with significant antemortem tooth loss to improve the number of measurements able to be taken.

Given the performance of the various methods on dry skulls and CT scans, it is recommended that in further studies and casework FORDISC 3.1 be used with caution to estimate ancestry from both dry skulls and CT scans, FORDISC 3.1 sex estimation be considered in conjunction with other sex estimation methods to ensure higher accuracy, and morphological assessment of sex and ancestry using CT scans should be utilized only when all traits in question are clearly visible. Measurements taken using cranial CT scans should be reliable as long as the necessary landmarks are visible and necessary angles are achievable using the viewing software. Finally, as with any sex or ancestry estimation, it is recommended that multiple methods be explored to compare and contrast results and ensure accuracy and consistency before making a final claim.

REFERENCES

Aalders M, Adolphi N, Daly B, Davis G, Boer HD, Decker S, Dempers J, Ford J, Gerrard C, Hatch G, Hofman P, Iino M, Jacobsen C, Klein W, Kubat B, Leth P, Mazuchowski E, Nolte K, Odonnell C, Thali M, Rijn RV, Wozniak K. 2017. Research in forensic radiology and imaging; Identifying the most important issues. Journal of Forensic Radiology and Imaging 8:1–8.

Aghayev E, Staub L, Dirnhofer R, Ambrose T, Jackowski C, Yen K, Bolliger S, Christe A, Roeder C, Aebi M, Thali MJ. 2008. Virtopsy – The concept of a centralized database in forensic medicine for analysis and comparison of radiological and autopsy data. Journal of Forensic and Legal Medicine 15:135–140.

Attia MH, Abulnoor BAE-S. 2020. Tailored logistic regression models for sex estimation of unknown individuals using the published population data of the humeral epiphyses. Legal Medicine 45:101708.

Attia MH, Abulnoor BAE-S. 2019. Sex estimation of femur using simulated metapopulation database: A preliminary investigation. Forensic Science International: Reports 1:100009.

Bakker BSD, Soerdjbalie-Maikoe V, Bakker HMD. 2013. The use of 3D-CT in weapon caused impression fractures of the skull, from a forensic radiological point of view. Journal of Forensic Radiology and Imaging 1:176–179.

Bass, W. M. (2005) *Human Osteology: A Laboratory and Field Manual*. 5th ed. Special Publication No. 2 of the Missouri Archaeological Society, Columbia, MO.

Bassed RB, Briggs C, Drummer OH. 2011. Age estimation using CT imaging of the third molar tooth, the medial clavicular epiphysis, and the spheno-occipital synchondrosis: A multifactorial approach. Forensic Science International 212.

Bhattacharyya K. 2016. Godfrey Newbold Hounsfield (1919-2004): The man who revolutionized neuroimaging. Annals of Indian Academy of Neurology 19:448.

Bertsatos A, Christaki A, Chovalopoulou M-E. 2019. Testing the reliability of 3D-ID software in sex and ancestry estimation with a modern Greek sample. Forensic Science International 297:132–137.

Bewes J, Low A, Morphett A, Pate FD, Henneberg M. 2019. Artificial intelligence for sex determination of skeletal remains: Application of a deep learning artificial neural network to human skulls. Journal of Forensic and Legal Medicine 62:40–43.

Brues AM. The once and future diagnosis of race. In: Gill G, Rhine S, editors. Skeletal attribution of race: methods for forensic anthropology. Maxwell Museum of Anthropological Papers No. 4. Albuquerque, NM: University of New Mexico, 1990;1–7.

Buikstra JE, Ubelaker DH. 1994. Standards for data collection from human skeletal remains. Arkansas Archeological Survey.

Carew RM, Errickson D. 2019. Imaging in forensic science: Five years on. Journal of Forensic Radiology and Imaging 16:24–33.

Carvallo D, Retamal R. 2020. Sex estimation using the proximal end of the femur on a modern Chilean sample. Forensic Science International: Reports 2:100077.

Caspari R. 2010. Deconstructing Race: Racial Thinking, Geographic Variation, and Implications for Biological Anthropology. In: Larsen CS, editor. A Companion to Biological Anthropology. Malden, MA: Wiley-Blackwell. p 104–123.

Cavalcanti MG, Haller JW, Vannier MW. 1999. Three-dimensional computed tomography landmark measurement in craniofacial surgical planning: Experimental validation in vitro. Journal of Oral and Maxillofacial Surgery 57:690–694.

Chege N, Sartoris DJ, Tyson R, Resnick D. 1996. Imaging Evaluation of Skull Trepanation Using Radiography and CT. International Journal of Osteoarchaeology 6:249–258.

Christensen A, Smith M, Gleiber D, Cunningham D, Wescott D. 2018. The Use of X-ray Computed Tomography Technologies in Forensic Anthropology. Forensic Anthropology 1:124–140.

Christensen AM, Hatch GM. 2019. Forensic fractography of bone using computed tomography (CT) scans. Journal of Forensic Radiology and Imaging 18:37–39.

Colman KL, Boer HHD, Dobbe JG, Liberton NP, Stull KE, Eijnatten MV, Streekstra GJ, Oostra R-J, Rijn RRV, Merwe AEVD. 2019. Virtual forensic anthropology: The accuracy of osteometric analysis of 3D bone models derived from clinical computed tomography (CT) scans. Forensic Science International 304:109963.

Combrinck N, Vuuren SJV. 2017. The role of post-mortem computed tomography in assault victims with head trauma in central South Africa. South African Journal of Radiology 21.

Cressey D. 2010. Pathologists scan for options beyond autopsies. Nature Medicine 16:1172–1172.

Curate F, Coelho J, Gonçalves D, Coelho C, Ferreira MT, Navega D, Cunha E. 2016. A method for sex estimation using the proximal femur. Forensic Science International 266.

Dedouit F, Telmon N, Costagliola R, Otal P, Joffre F, Rougé D. 2007. Virtual anthropology and forensic identification: Report of one case. Forensic Science International 173:182–187.

Dedouit F, Savall F, Mokrane F-Z, Rousseau H, Crubézy E, Rougé D, Telmon N. 2014. Virtual anthropology and forensic identification using multidetector CT. The British Journal of Radiology 87:20130468.

Dudzik B, Jantz RL. 2016. Misclassifications of Hispanics Using FORDISC 3.1: Comparing Cranial Morphology in Asian and Hispanic Populations. Journal of Forensic Sciences 61:1311–1318.

Elliott M, Kurki H, Weston DA, Collard M. 2014. Estimating fossil hominin body mass from cranial variables: An assessment using CT data from modern humans of known body mass. American Journal of Physical Anthropology 154:201–214.

Elliott M, Collard M. 2009. FORDISC and the Determination of Ancestry from Cranial Measurements. Biology Letters 5:849–852.

Franklin D, Flavel A, Kuliukas A, Cardini A, Marks MK, Oxnard C, O'Higgins P. 2012. Estimation of sex from sternal measurements in a Western Australian population. Forensic Science International 217.

Garvin HM, Sholts SB, Mosca LA. 2014. Sexual dimorphism in human cranial trait scores: Effects of population, age, and body size. American Journal of Physical Anthropology 154:259–269.

Gill, GW. 1998. Craniofacial criteria in the skeletal attribution of race. In *Forensic Osteology: Advances in the Identification of Human Remains* (2nd Ed.) ed. by K. Reichs, pp. 293-315. Charles C Thomas, Springfield, IL.

Giurazza F, Vescovo RD, Schena E, Battisti S, Cazzato RL, Grasso FR, Silvestri S, Denaro V, Zobel BB. 2012. Determination of stature from skeletal and skull measurements by CT scan evaluation. Forensic Science International 222.

Guyomarc'H P, Bruzek J. 2011. Accuracy and reliability in sex determination from skulls: A comparison of FORDISC® 3.0 and the discriminant function analysis. Forensic Science International 208.

Hauser G, De Stefano GF. 1989. Epigenetic variants of the human skull. Stuttgart: E. Schweizerbart'sche Verlagsbuchhandlung.

Hefner JT. 2009. Cranial Nonmetric Variation and Estimating Ancestry. Journal of Forensic Sciences 54:985–995.

Hefner JT, Ousley SD. 2014. Statistical Classification Methods for Estimating Ancestry Using Morphoscopic Traits. Journal of Forensic Sciences 59:883–890.

Herrera MD, Tallman SD. 2019. Craniometric variation and ancestry estimation in two contemporary Caribbean populations. Forensic Science International 305:110013.

Hishmat AM, Michiue T, Sogawa N, Oritani S, Ishikawa T, Hashem MAM, Maeda H. 2014. Efficacy of automated three-dimensional image reconstruction of the femur from postmortem computed tomography data in morphometry for victim identification. Legal Medicine 16:114–117.

Inoue M. 1990. Fourier analysis of the forehead shape of skull and sex determination by use of computer. Forensic Science International 47:101–112.

Jantz, R. and S. Ousley (2005) *FORDISC 3.1*. University of Tennessee Press, Knoxville, TN.

Johnson D, Ohiggins P, Moore W, Mcandrew T. 1990. Determination of race and sex of the human skull by discriminant function analysis of linear and angular dimensions — an appendix. Forensic Science International 45:1–3.

Joshi M, Mishra B, Lalwani S, Kumar A, Kumar A, Kumar S, Gupta A, Sagar S, Singhal M, Panda A, Rattan A. 2018. A comparative analysis of the findings of postmortem computed tomography scan and traditional autopsy in traumatic deaths: Is technology mutually complementing or exclusive? Archives of Trauma Research 7:24.

Katsumura S, Sato K, Ikawa T, Yamamura K, Ando E, Shigeta Y, Ogawa T. 2016. "High-precision, reconstructed 3D model" of skull scanned by conebeam CT: Reproducibility verified using CAD/CAM data. Legal Medicine 18:37–43.

Klales AR. 2020. MorphoPASSE: Morphological pelvis and skull sex estimation program. Sex Estimation of the Human Skeleton:271–278.

Klales AR, Ousley SD, Vollner JM. 2012. A revised method of sexing the human innominate using Phenice's nonmetric traits and statistical methods. American Journal of Physical Anthropology 149:104–114.

Krogman WM, İşcan MY. 1986. The human skeleton in forensic medicine. Springfield, IL: Charles C. Thomas, 1986.

Langley NR, Meadows Jantz L, Ousley SD, Jantz RL, Milner G. 2016. Data Collection Procedures for Forensic Skeletal Material 2.0. Knoxville: University of Tennessee.

Little MA, Sussman RW. 2010. History of Biological Anthropology. In: Larsen CS, editor. A Companion to Biological Anthropology. Malden, MA: Wiley-Blackwell. p 13–38.

Lo Re G, Salerno S, Terranova MC, Argo A, Lo Casto A, Zerbo S, Lagalla R. 2019. Virtopsy and Living Individuals Evaluation Using Computed Tomography in Forensic Diagnostic Imaging. Seminars in Ultrasound, CT and MRI 40:67–78.

Mall G, Hubig M, Büttner A, Kuznik J, Penning R, Graw M. 2001. Sex determination and estimation of stature from the long bones of the arm. Forensic Science International 117:23–30.

Marchewka J, Skrzat J, Wróbel A. 2014. Analysis of the enamel hypoplasia using micro-CT scanner versus classical method. Anthropologischer Anzeiger 71:391–402.

Moore MK, Digangi EA, Ruíz FPN, Davila OJH, Medina CS. 2016. Metric sex estimation from the postcranial skeleton for the Colombian population. Forensic Science International 262.

Neubauer S, Gunz P, Weber GW, Hublin J-J. 2012. Endocranial volume of Australopithecus africanus: New CT-based estimates and the effects of missing data and small sample size. Journal of Human Evolution 62:498–510.

Ozgen A, Ariyurek M. 1998. Normative measurements of orbital structures using CT. American Journal of Roentgenology 170:1093–1096.

Patterson M, Tallman S. 2019. Cranial and Postcranial Metric Sex Estimation in Modern Thai and Ancient Native American Individuals. Forensic Anthropology 2.

Phenice TW. 1969. A newly developed visual method of sexing the os pubis. American Journal of Physical Anthropology 30:297–301.

Rai A, Acharya A, Naikmasur V. 2016. Age estimation by pulp-to-tooth area ratio using cone-beam computed tomography: A preliminary analysis. Journal of Forensic Dental Sciences 8:150.

Ramsthaler F, Kettner M, Gehl A, Verhoff M. 2010. Digital forensic osteology: Morphological sexing of skeletal remains using volume-rendered cranial CT scans. Forensic Science International 195:148–152.

Relethford JH. 2010. Race and Conflicts within the Profession of Physical Anthropology During the 1950s and 1960s. In: Little MA, Kennedy KAR, editors. Histories of American Physical Anthropology in the Twentieth Century. Plymouth, UK: Lexington Books. p 207–219.

Rhine S. 1990. Non-metric skull racing. In: Gill GW and Rhine S, editors. Skeletal Attribution of Race: Methods for Forensic Anthropology. Maxwell Museum of Anthropology, Anthropological Papers No. 4. p. 9-20.

Rogers TL. 1999. A Visual Method of Determining the Sex of Skeletal Remains Using the Distal Humerus. Journal of Forensic Sciences 44.

Simmons-Ehrhardt TL, Ehrhardt CJ, Monson KL. 2019. Evaluation of the suitability of cranial measurements obtained from surface-rendered CT scans of living people for estimating sex and ancestry. Journal of Forensic Radiology and Imaging 19:100338.

Spradley MK, Jantz RL. 2011. Sex Estimation in Forensic Anthropology: Skull Versus Postcranial Elements. Journal of Forensic Sciences 56:289–296.

Stini WA. 2010. Sherwood L. Washburn and "The New Physical Anthropology". In: Little MA, Kennedy KAR, editors. Histories of American Physical Anthropology in the Twentieth Century. Plymouth, UK: Lexington Books. p 173-185.

Stocking GW. 1988. Bones, Bodies, Behavior. In: Bones, bodies, behavior: essays on biological anthropology. Madison, WI: University of Wisconsin Press. p 3–17.

Stull KE, Tise ML, Ali Z, Fowler DR. 2014. Accuracy and reliability of measurements obtained from computed tomography 3D volume rendered images. Forensic Science International 238:133–140.

Tallman S. 2019. Cranial Nonmetric Sexual Dimorphism and Sex Estimation in East and Southeast Asian Individuals. Forensic Anthropology 2.

Tallman SD, Blanton AI. 2020. Distal Humerus Morphological Variation and Sex Estimation in Modern Thai Individuals. Journal of Forensic Sciences 65:361–371.

Thali MJ, Yen K, Schweitzer W, Vock P, Boesch C, Ozdoba C, Schroth G, Ith M, Sonnenschein M, Doernhoefer T, Scheurer E, Plattner T, Dirnhofer R. 2003. Virtopsy, a New Imaging Horizon in Forensic Pathology: Virtual Autopsy by

Postmortem Multislice Computed Tomography (MSCT) and Magnetic Resonance Imaging (MRI)—a Feasibility Study. Journal of Forensic Sciences 48:2002166.

Thompson TJU. 2005. Heat-induced Dimensional Changes in Bone and their Consequences for Forensic Anthropology. Journal of Forensic Sciences 50:1–8.

Uthman AT, Al-Rawi NH, Al-Naaimi AS, Tawfeeq AS, Suhail EH. 2010. Evaluation of frontal sinus and skull measurements using spiral CT scanning: An aid in unknown person identification. Forensic Science International 197.

Vance VL, Steyn M, L'Abbé EN. 2011. Nonmetric Sex Determination from the Distal and Posterior Humerus in Black and White South Africans. Journal of Forensic Sciences 56:710–714.

Villa C, Olsen K, Hansen S. 2017. Virtual animation of victim-specific 3D models obtained from CT scans for forensic reconstructions: Living and dead subjects. Forensic Science International 278.

Villa C, Lynnerup N. 2012. Hounsfield Units ranges in CT-scans of bog bodies and mummies. Anthropologischer Anzeiger 69:127–145.

Waitzman AA, Posnick JC, Armstrong DC, Pron GE. 1992a. Craniofacial Skeletal Measurements Based on Computed Tomography. Part I. Journal of Craniofacial Surgery 3:182.

Waitzman AA, Posnick JC, Armstrong DC, Pron GE. 1992b. Craniofacial Skeletal Measurements Based on Computed Tomography: Part II. Normal Values and Growth Trends. The Cleft Palate-Craniofacial Journal 29:118–128.

Walker PL. 2005. Greater sciatic notch morphology: Sex, age, and population differences. American Journal of Physical Anthropology 127:385–391.

Walker PL. 2008. Sexing skulls using discriminant function analysis of visually assessed traits. American Journal of Physical Anthropology 136:39–50.

Washburn SL. 1951. Section ozahnf Anthropology: The New Physical Anthropology*. Transactions of the New York Academy of Sciences 13:298–304.

White TD, Black MT, Folkens PA. 2012. Assessment of Age, Sex, Stature, Ancestry, and Identity of the Individual. In: Human Osteology. 3rd ed. Burlington, MA: Academic Press. p 379–427.

Zech W-D, Hatch G, Siegenthaler L, Thali MJ, Lösch S. 2012. Sex determination from os sacrum by postmortem CT. Forensic Science International 221:39–43.

Zhan M-J, Cui J-H, Zhang K, Chen Y-J, Deng Z-H. 2019. Estimation of stature and sex from skull measurements by multidetector computed tomography in Chinese. Legal Medicine 41:101625.

Zheng J, Liu X, Chen X, Jiang W, Abdelrehem A, Zhang S, Chen M, Yang C. 2019. Customized skull base–temporomandibular joint combined prosthesis with 3D-printing fabrication for craniomaxillofacial reconstruction: a preliminary study. International Journal of Oral and Maxillofacial Surgery 48:1440–1447.

CURRICULUM VITAE

[redacted]